1. Introduction

1.1 The mechanism of plant reproduction

In response to fluctuating environmental conditions, animal responses are primarily behavioral and physiological on a short-term scale. However, in higher plants including *Arabidopsis thaliana*, have adopted evolutionarily complex growth strategies; subsequent development for longer term acclimation to a variable environment, rather than behavior (Chasan and Walbot, 1993). One of the most striking differences between the developmental approaches of plants and animals is that, in plants, several mitotic divisions intervene between meiosis and gamete formation (Chasan and Walbot, 1993).

In flowering plants, reproductive development begins with the transition of the apical meristem from vegetative tissue to produce inflorescence branches including flowers. To switch from vegetative to reproductive development, the apical meristem must integrate long-range signal. Then, primordia begin to differentiate into mature floral organs. The formation of floral organs including spores

and gametes plays a critical role in sexual reproduction and is tightly controlled (Bernier and Perilleux, 2005).

The flowers of the sporophyte, do not produce gametes directly. Instead, meiotic divisions within the sexual organs of the flower give rise to haploid megaspores and microspores, which undergo several mitotic divisions to produce the gametophytes.

1.1.1 Formation of female gamete

In specialized apical portion of the ovary placenta, primordium including a single diploid megaspore mother cell (MMC) is derived. The developmental processes of the embryo sac can be divided into two stages called megasporogenesis and megagametogenesis. Megasporogenesis begins with the meiotic division of MMC, giving rise to four haploid megaspores. Subsequently, the three megaspores at the micropylar pole degenerate and only one surviving functional megaspore (FM) enters the process of megagametogenesis. After the first mitosis, the two nuclei migrate to opposite poles and a large central vacuole is seen (FG2). It is assumed that this vacuole plays an important role in positioning the nuclei (Cass et al., 1985). Two additional mitotic divisions are

needed for generating the eight-nucleate embryo sac. Functional megaspore undergoes three rounds of mitosis without cytokinesis. However, immediately following the third mitosis, cell walls form and partition the nuclei into cellular compartments (Pischke et al., 2002). At this FG5 stage, the eight nuclei migrate according to their cell-fate specifications and differentiate into the each cell they give rise to. After cellularization, centrally located two polar nuclei will fuse to form a homo-diploid central cell (FG6). The central cell gives rise to triploid primary endosperm nucleus after fertilization with a sperm nucleus. The egg cell is located opposite to the antipodal cell at the micropylar end of the embryo sac and fuses with a sperm to form a zygotic embryo. The two most distal nuclei, at the micropylar pole, will differentiate into the synergid cells that are on either side of the egg cell. Three antipodal cells are located at the chalazal end of the embryo sac. After cellularization and fusion of the two polar nuclei, the three antipodal cells degenerate and the mature female gamete is formed (FG7).

1.1.2 Formation of male gamete

Male reproductive process in *Arabidopsis* takes place in the

stamen. Similar to the female gametophyte development, male gametogenesis begins with the meiotic division of a diploid pollen mother cell (PMC). PMC gives rise to a tetrad of haploid cells after meiotic division. Then, the individual four haploid cells are released as microspores. Unlike the female megaspores, all microspores survive and undergo asymmetric mitotic division, each producing a pollen grain containing two cells: a larger vegetative cell and a smaller generative cell that is engulfed in the cytoplasm of a vegetative cell. Only the generative cell undergoes a second mitosis to form two identical sperm cells. The vegetative nucleus gives rise to the pollen tube after pollination, delivering two sperm cells to the ovule.

1.2 Previous studies for isolation of gametophytic mutants

For more than a century, diverse studies using forward or reverse genetics have been carried out to identify genes that function in gametogenesis. For some of the identified genes, the mutants have defects in different developmental stages of either the embryo sac (Christensen et al., 2002; Drews and Yadegari, 2002;

Grini et al., 2002; Johnston et al., 2007; Johnston et al., 2008) or the pollen grain (Lalanne et al., 2004; Kim et al., 2008; Brownfield et al., 2009). However, about 46% of the mutations cause defects in both female and male gametophyte formation, including essential cellular processes such as mitosis, vacuole formation, cellularization, nuclear migration and cell expansion (Pagnussat et al., 2005). It suggests that many of the major events of gametogenesis could be general and regulated in the male and the female gametophytes by the same gene products. Thus, mutation in genes encoding proteins required for some of these essential events are likely to affect both female and male gametophyte development of function. The post-meiotic successive mitoses and cytokinetic patterns that exist only in flowering plants are critical to the plant life cycle; yet, the information and mechanisms of genes governing the major events of both mega- and microgametogenesis are largely unknown.

1.3 Microtubule organization during gametogenesis

In higher plants like *Arabidopsis*, mitosis and following cytokinesis take place without structurally defined microtubule organizing centers (MTOC). Instead, the nuclear envelope itself

appears to act as a MTOC for microtubule nucleation and spindle organization (Canaday et al., 2000). Mutations in genes required for regulating microtubule organization are often shown to be homozygous lethal (Park et al., 1998; Zeng et al., 2009). For years, γ-tubulin is well known microtubule-interacting factor as a key regulator of microtubule dynamics (Job et al., 2003). Moreover, in developing gametophyte lacking essential genes like γ-tubulin, the spindle array and cytokinesis collapse and fail to take place (Pastuglia et al., 2006).

Plant cytokinesis is primarily dependent on microtubules (Guertin et al., 2002). The phragmoplast, an array of microtubules following anaphase, have a critical role in the formation of the cell plate. In the phragmoplast, microtubules are rearranged in two mirrored sets: their plus ends are juxtaposed at the division site and their minus ends face the reforming nuclei. These phragmoplast arrays serve as tracks for Golgi-mediated transportation toward microtubule plus ends. Thus, the arrangement of this antiparallel array of microtubule allows vesicles to be delivered toward microtubule plus ends, to the division site (Lee et al., 2007).

In pollen development, the nuclear division of meiosis I is not followed by cytokinesis (McCormick, 1993). Instead, cytokinesis begins at the end of meiosis II simultaneously to demarcate each

microspore (Yang et al., 2003). This enables the two mutant haploid microspores to share the cytoplasm with the two wild-type haploid microspores inherited from the heterozygous parent (Liu et al., 2011).

Cytokinesis is also important for female gametophyte development. At FG5 stage of ovule, the eight nuclei migrate according to their cell-fate specifications. Although the mechanism of the nuclear migration is not well understood, a large concentration of radiating microtubules which function in the migration and arrangement of the nuclei appear to establish and maintain organelle polarity during cellularization (Huang and Sheridan, 1994; Webb and Gunning, 1994).

1.4 Nuclear pore proteins in *Arabidopsis*

The basic architecture of the nuclear pore complexes (NPCs), the largest multi-protein complex in the cell, is conserved among vertebrates, yeast and plants (Allen and Douglas, 1989; Goldberg and Allen, 1996; Fiserova et al., 2009). NPCs are important structures embedded in the nuclear envelope (NE) that mediate the macromolecular exchange between the nucleus and cytoplasm

(Meier and Brkljacic, 2009). NPCs are stable throughout interphase but are dynamic during cell division; they disassemble into subcomplexes during mitosis and are recruited to the newly-formed NEs at the end of the cell cycle (Daigle et al., 2001; Dultz et al., 2008). Approximately 30 different proteins termed nucleoporin (NUP) compose NPC, and the overall structures of both NUPs and NPC are well characterized in vertebrates and yeast (Brohawn et al., 2009; Brohawn and Schwartz, 2009; Elad et al., 2009). Compared to human and yeast studies where detailed information is available for certain NUPs, only about a dozen NUPs in plants had been identified and characterized until now (Braud et al., 2012). Tamura et al. (2010) took an interactive proteomic approach and found that the plant NPC also contains at least 30 NUPs including plant specific NUPs in addition to NUPs showing similar domains and sequence homologies to those in humans and yeast.

NUPs contain a very limited set of domains: WD40 domain and FG repeat domain. The WD repeats family form a ß-propeller structure that is thought to be important for assembly of protein complexes (Smith et al., 1999). FG repeats, the most common domains found in NUPs, are responsible for nuclear pore

permeability for controlling transport. However, the biological functions of many plant NUPs remain unknown.

1.5 Nucleoporins for a successful mitosis

During mitosis the NPC appears to disassemble in stages. Although some nuclear envelope components are retained in the mitotic ER network during cell division, numerous other ones localize to mitotic structures and play crucial roles in consecutive stages of the division process (Dultz et al., 2008; Lupu et al., 2008). Evidence from several organisms demonstrates that nucleoporins and their subcomplexes play a variety of important roles in mitosis.

The Nup107−160 nuclear pore subcomplex, the largest subcomplex of the NPC in human cells, *Xenopus* and *C. elegans*, is recruited to kinetochores early in mitosis, and is required for efficient kinetochore attachment to microtubules (Loiodice et al., 2004; Rasala et al., 2006; Franz et al., 2007). Nup358, known as RanBP2, also accumulates at free spindle ends and free kinetochores and is required for chromosome alignment and spindle formation. Accumulation of mitotic cells with multipolar spindles and unaligned chromosomes were caused by the mutation of Nup358

(Salina et al., 2003; Joseph et al., 2004). The nucleoporin TPR (Translocated Promoter Region) is one of the main components in the nuclear basket of the NPC (Frosst et al., 2002). Tpr and its homologs in humans, *drosophila*, metazoans and fungi, associates with the dynein light chain, recruiting spindle assembly checkpoint proteins to promote progress through anaphase (Nakano et al., 2011). In HeLa cell, Tpr with dynein and dynactin, both function as a spatial and temporal regulator of spindle checkpoint during cell division (Nakano et al., 2010). One of the key players in mitosis appears to be nucleoporin RNA export 1 (Rae1), which often acts in a subcomplex with Nup98 both in interphase and mitosis (Matsuoka et al., 1999). Rae1/Nup98 binds to, and regulates, the activity of the APC (Anaphase Promoting Complex) in mice, stalling mitosis progression until chromosomes are properly attached to the spindle (Jeganathan et al., 2005). Haploinsufficiency of both proteins results in premature sister chromatin separation and aneuploidy (Jeganathan et al., 2005). In HeLa cells, Rae1 binds to the nuclear mitotic apparatus (NuMA), which forms a complex with cytoplasmic dynein. Rae1/NuMA coupled with dynein motor protein is critical for tethering microtubules at the spindle poles and is required for bipolar spindle formation (Merdes et al., 1996; Blower et al., 2005; Wong et al., 2006).

Whilst detailed information is available for certain NUPs in human and yeast studies, only about a dozen NUPs in plants had been identified and characterized (Braud et al., 2012). Among them, Rae1 was shown to co-localizes with tubulin and binds directly to microtubules, which is required for proper spindle assembly and chromosome segregation (Lee et al., 2009).

1.6 Nup88 homologs in other organisms

The NPC is well characterized in vertebrates and yeast, and their nucleoporins share structural motifs and specific sequences. These can be grouped into three main categories: scaffold nucleoporins, the main structural components of the NPC; nucleoporins embedded in the membrane that tether the scaffold nucleoporins; and barrier nucleoporins. The latter group regulate the selective permeability of the pore, via their long phenylalanine-glycine dipeptide-domains, or FG repeats (Strambio-De-Castillia et al., 2010; Onischenko and Weis, 2011).

MOS7 is a non-FG repeat protein, however its homologue, Nup88, is known to form a complex via its C-terminal domain with FG protein Nup214 in yeast, Drosophila and human cells (Bernad et al., 2006). Nup214 formed complexes with Nup88 and CRM1 in vivo

and Nup214 protected Nup88 from degradation at the nuclear rim. The major function of Nup88/Nup214 complex is to regulate nuclear protein export (Bernad et al., 2006), promoting the retention of specific immunity regulators in the nucleus, in concert with nuclear export factor CRM1 (Roth et al., 2003; Xylourgidis et al., 2006).

Recent studies on MOS7 have revealed that the function of Nup88 is also conserved between plants and animals since Nup88s in *Drosophila*, human and plant are critical for the regulation of innate immunity (Uv et al., 2000; Roth et al., 2003; Cheng et al., 2009). Mutants in *members only* (*mbo*), encoding the *Drosophila* Nup88, fail to accumulate the Rel proteins Dif and Dorsal in the nucleus and also fail to activate their immune response (Uv et al., 2000; Roth et al., 2003; Xylourgidis et al., 2006). In *Arabidopsis*, MOS7/Nup88 is required for nuclear accumulation of the R protein snc1, as well as the key immune regulators EDS1 and NPR1. MOS7 promotes nuclear retention and accumulation of autoactive snc1 as a critical process in the constitutive activation of immune responses.

In human cell, Nup88 has been proposed as a tumor marker. Hashizume noted that overexpression of Nup88 in human enhanced multinucleated cell formation and RNAi-mediated knockdown of Nup88 disrupted Nup214 expression and localization and caused multipolar spindle phenotypes (Hashizume et al., 2010).

1.7 Purpose of the study

In order to identify genes involved in reproduction of *Arabidopsis*, about 80,000 T-DNA activation tagging mutant lines were screened for showing ovule and seed abortion phenotypes. One of the identified mutants was the *mos7-5*, in which the T-DNA inserted into *MOS7 (Modifier Of Snc1,7)* —a gene that is homologous to human and *Drosophila melanogaster* nucleoporin *Nup88*. Within the *mos7* mutant group, *mos7-1*, a partial *MOS7*-loss-of-function mutant (four amino acids in-frame deletion), was originally identified by Cheng et al. (2009) as a suppressor of *snc1* (suppressor of npr1-1, constitutive). The *snc1* mutant exhibited constitutive activation of the defense R protein snc1 and showed a stunted nature. A *mos7-1* homozygous mutation suppresses not only immune responses, but also the mutants exhibits phenotypic defects caused by *snc1* mutation, demonstrating that MOS7-mediated nucleocytoplasmic passage of defense proteins plays an important role in plant innate immunity (Cheng et al., 2009). However, MOS7 function during normal development has not been thoroughly examined mainly because there was no discernible developmental phenotype observed in *mos7-1* homozygous mutants.

Recently, Hashizume at al. (2010) reported that alterations in human Nup88 expression were linked to the progression of carcinogenesis, multinucleated cells, and the multipolar spindle phenotype as a tumor marker. Thus, MOS7 might have important roles during cell division in plant cells as well. In this report, I examine the critical role of a functional homolog of Nup88 of human – *Arabidopsis* MOS7 – in cell division during gametogenesis and embryogenesis through proper cytoskeleton modulation.

2. MATERIALS AND METHODS

2.1 Plant materials and growth conditions

Arabidopsis thaliana Columbia-0 (Col-0) was used as the wild-type. The *mos7-5* null mutant was isolated from an activation tagging mutant library and was backcrossed to wild-type five times before analyses. *mos7-2*, *mos7-3* and *mos7-4* alleles were from the ABRC, Ohio State University. *Arabidopsis* plants were grown in a long-day (16 h light/8 h dark) photoperiod under cool white fluorescent light (100 μmole/m^2/s) at 22°C with 60% relative humidity.

2.2 Seed-set analysis and whole-mount clearing

Siliques (DAP 8 to 10) were dissected on a stereoscope, and then the number of normal seeds, aborted seeds and undeveloped ovules was counted. For whole mount clearing, siliques (DAP 1 to 8) and pistils of FG7 stage were dissected, and seeds and ovules were mounted in clearing solution (2.5g chloral hydrate; 0.3ml 100% glycerol; 0.7ml distilled water). After incubation for several hours, samples were observed using an Axio Imager A1 microscope (Carl

Zeiss) under DIC optics and were photographed using an AxioCam HRc camera (Carl Zeiss).

2.3 Pollen viability analysis

For Alexander staining for pollen viability, stamens from mature flowers were placed on a microscopic slide. A few drops of Alexander stain buffer (95% ethanol, 10mL; Malachite green (1% in 95% ethanol), 1mL; Fuchsin acid (1% in water), 5mL; Orange G (1% in water), 0.5mL; phenol, 5g; chloral hydrate, 5 g; glacial acetic acid, 2mL; glycerol, 25mL; distilled water, 50mL) were added. The detail method for analyzing pollen viability was performed as described previously (Schoft et al., 2011).

2.4 Confocal laser scanning microscopic analysis

For the analysis of embryo sac development in wild-type and the *mos7-5* mutant, CLSM of ovules was performed as previously described (Christensen et al., 1997) with slight modifications. Pistils of floral stage 6 to stage 12 were harvested. For fixation, dissected ovules were dipped in 4% glutaraldehyde (in 12.5mM cacodylate, pH 6.9) under vacuum (~200 torr) for 20min. A conventional ethanol series with 10 min. per step was followed by

dehydration and the tissue was subsequently cleared in 2:1 benzyl benzoate:benzyl alcohol. After mounting with immersion oil, samples were observed with a LSM700 (Carl Zeiss).

2.5 Recombinant plasmid construction

To generate *Pro2.8Kb:cMOS7:GUS* construct for genetic complementation of the *mos7-5* phenotype, a 5.2kb fragment containing the full-length cDNA of *MOS7* (2.4kb) plus the 5' upstream region (2.8kb) was cloned into a *pBI101* vector. To generate *Pro2.0Kb:MOS7:GFP* construct, *a* portion of the *MOS7* gene, 2.0kb of 5' upstream sequences plus 4.1 kb of the *MOS7* coding region, was cloned into a *pBI-GFP* (S65T) vector. For partial domain complementation analysis, a 4.2kb partial *MOS7* gene containing the 5' upstream sequences (2.0kb) plus 2.2kb of N-terminal region was cloned into a *pPZP211* vector (*Pro2.0Kb:MOS7-N*). To generate *Pro2.0Kb:MOS7:RFP* construct, PCR amplified DNA containing the mRFP sequence was subcloned into *SacI* and *BamHI* sites in the pBI101.2 vector (*pBI-mRFP*). And the 2.0kb of 5' upstream sequences plus 4.1kb of the *MOS7* coding region was cloned into *SalI* and *BamHI* sites in the *pBI-mRFP* vector. To generate a *ProCYCB1;1:CYCB1;1:GFP* construct,

a genomic fragment including 1.1kb of putative promoter and 0.7kb of the coding sequence of *CYCB1;1* containing the mitotic Destruction Box (D-box) was cloned into a *pBI-GFP* vector as described by Eloy et al. (2011). This transgene was directly transformed into *MOS7/mos7-5* heterozygous plants.

2.6 Quantitative PCR and RT-PCR

For expression analysis of *MOS7* in wild-type, two week-old seedlings, the following plant parts were collected: influorescence including floral stage 1 to 13, leaf, roots, seeds at torpedo stage, mature pistil, and mature pollen. For expression analysis of *MOS7* at the 4^{th} and 9^{th} exons, floral buds with floral stage 1 to 10 were collected. Total RNAs were extracted using liquid nitrogen and RNAqueous^{TM} (Ambion). After DNase-I treatment, the first-strand cDNA was synthesized using the QuantiTect Reverse Transcription Kit (Qiagen). quantitative RT-PCR product was amplified using the iQ SYBR Green Supermix (Bio-Rad) on a CFX96 machine (Bio-Rad), and the data were analyzed using CFX Manager software (Bio-Rad). Relative transcript levels were determined by normalization of the resulting expression levels to that of *TUB2*. To identify the genotype of the aborted seeds, genomic DNAs were

extracted from aborted seeds with DAP 8 to 10, and qPCR was performed using primer sets for T-DNA and *TUB* amplification. The resulting qPCR from two week-old *MOS7/mos7-5* seedlings was used as an internal control in which half of the genomic DNA carries the *mos7-5* allele. To shed light on the phenomenon of high level of T-DNA transmission efficiency in *MOS7/mos7-5* plants, qPCR was performed using genomic DNAs extracted from viable pollen grains of *qrt/qrt MOS7/mos7-5* plants. Total genomic DNAs were extracted from all four viable 4-pollen and two viable 2-pollen after removing the two attached dead pollen manually and qPCR was performed as above. The primer sequences for quantitative RT-PCR are listed in the Table 1.

2.7 GUS and GFP expression and DAPI analysis

GUS histochemical analysis was performed as previously described (Yadegari et al., 2000). Histochemical localization of GUS activity in *Pro2.8Kb:cMOS7:GUS* transgenic plants was performed on intact pistils, which were excised longitudinally, vacuum-infiltrated for 10 to 15 min on ice with staining solution (50mM sodium phosphate buffer, pH 7.0, 0.2% Triton X-100, 10mM potassium ferrocyanide, 10mM potassium ferricyanide, and 1mM

X-gluc), and incubated for 12 to 16hr at 37°C. Individual ovules were then dissected out, mounted in 50mM sodium phosphate buffer, pH 7.0, and observed using an Axio Imager A1 microscope (Carl Zeiss) under DIC optics and were photographed using an AxioCam HRc camera (Carl Zeiss).

Individual ovules from *Pro2.0Kb:MOS7:GFP* transgenic plants were dissected out, mounted in water, and then analyzed using LSM700 (Carl Zeiss) CLSM. For DAPI staining, detached stamens from the plants expressing MOS7-GFP fluorescence were collected into a DAPI staining solution (1 μg/mL in 1X PBS). DAPI-stained pollen samples were analyzed using LSM700 (Carl Zeiss) CLSM.

2.8 Yeast two hybrid assay

For MOS7 interaction, full-length c*MOS7* (2.4kb), N-terminal region of *MOS7* (0.8kb) and C-terminal of *MOS7* (0.8kb) cDNA were cloned into a *pGBKT7* bait vector with *TRP1* as a selection marker in yeast YH109 cells. Candidate binding proteins were cloned into a *pGADT7* prey vector with *Leu* as a selection marker in the Matchmaker Two-Hybrid system (Clontech). Assay conditions were as described by the manufacturer. From the transformed yeast colonies of each combination, I chose eight independent

colonies and examined their growth on −Leu/−Trp/−Ade/−His/ quadruple dropout media to determine interactions. A representative single colony was diluted with water and spotted on new quadruple dropout media to photograph. A yeast two hybrid screening with MOS7 was performed by Panbionet Corp. (www.panbionet.com), using the yeast strain AH109. See Table 2 for a list of plasmid constructed and primer sequences used.

2.9 BiFC

For MOS7 interaction, full−length c*MOS7* (2.4 kb), c*Dynein* (0.4 Kb) and c*Kinectin* (1.0 kb) cDNA were cloned into a *pSAT4−nEYFP−C1* and *pSAT4−cEYFP−C1−B* vector reciprocally. 16−24 h transient expression after introduction in pairs into *Arabidopsis* protoplasts by PEG transfection, protein−protein interactions were determined by LSM700 confocal microscopy (Carl Zeiss).

2.10 Protein gel blotting analysis

Floral stage 6 to 10 floral buds of wild−type and *MOS7/mos7*−5 plants carrying the *ProCYCB1;1:CYCB1;1:GFP* construct were harvested and stored in liquid nitrogen, and proteins were subsequently extracted by homogenizing the samples in protein

extraction buffer (50mM Tris-Cl, pH7.5; 100mM NaCl; 10mM $MgCl_2$; 1mM EDTA; 1mM DTT; 1mM PMSF; 10% glycerol and 1X Complete Protease Inhibitor (Brownell et al.)). After the supernatants were quantified using a protein assay kit (Bid-Rad), equivalent amounts of protein were loaded in SDS-PAGE and were transferred onto nitrocellulose membrane. Following blocking, the membrane was incubated with primary mouse anti-GFP antibody (Santa Cruz). After incubation with secondary goat HRP-coupled antibody (Santa Cruz), detection of HRP was performed using a Lumigen TMA-6 kit (GE Healthcare) by ImageQuant LAS 4000 machine (GE Healthcare).

Table 1. List of primer sequences used for quantitative PCR and RT-PCR

Gene	Primer pairs	Nucleotide sequences
MOS7 (1th exon)	MOS7 2nd F	CTTCCTCCCAAGATGAACCC
	MOS7 2nd R	GCGCAGAGATAATCGGTGAAG
MOS7 (4th exon)	3.5 MOS7 F	CAGATACTGAGCTACCAGAG
	05680.3 R	CTATCCCACAGATGATCTCC
MOS7 (7th exon)	MOS7 6th F	GGTTGATGAAATCCAGCCTG
	05680 R	GAGCGGCAGGTTTGAAGTTG
MOS7 (8th exon)	MOS7 7th F	GCTTTACCTAACCAGCGTTC
	05680.1 qRT R	CAGTTCTGCTCTCGTCAGAG
MOS7 (9th exon)	05680.2 qRT F	CAATGCTTGCAACGTCTCCG
	05680.2 qRT R	GGATGATTGAAGCGCATCCAC
MOS7 (T-DNA PCR)	65033 T-Left	TGCTCTGGTAGCTCAGTATC
	LB3	TTGACCATCATAACTCATTGCTG
MOS7 (WT PCR)	65033 T-Left2	CCACCTTCACTATCAGCCG
	65033 T-Right2	GGTTCAGAAATCTATACTAG
TUB	TUB real F	ATCGATTCCGTTCTCGATGT
	TUB real R	ATCCAGTTCCTCCTCCCAAC
ACT	ACT1 F	TCTTGATCTTGCTGGTCGTG
	ACT1 R	AATGGTGATCACTTGCCCATC
CYCB1;1	sGFP-F	AGATCTATGGTGAGCAAGGGCGAGGAG
	YB40	GGTGGTGCAGATGAACTTCA
At5g05660	At5g05660.2 qRT F	CTGGCATTTATGATTCCTGC
	At5g05660.2 qRT R	CCTTGAGACTTGCAGGATTG
At5g05670	At5g05670.2 qRT F	CCACTTCCGGTCAGCCCAG
	At5g05670.2 qRT R	GGCTGAGCAGTGGTCGCATC
At5g05690	At5g05690 F	CAGAGAGTGCAACCCTAGCC
	At5g05690 R	CGCTACGAGTGGCTAACATC
At5g05700	At5g05700 F	CAAGCATCGGCCTTGCTAC
	At5g05700 R	GGGATCCAGACTATGCATTC

Table 2. List of plasmid constructed and primer sequences used

Plasmid	Primer 1	Primer 2
Pro2.0Kb:MOS7:GFP	GGGTCGACCCATGGCAA TGCCTCATTTTC	GGGGATCCTCCGCCACCG CCTCCACCCATGAAACTG CTTTCTTGCG
Pro2.0Kb:MOS7:RFP	RFP:GCGGGATCCATGGC CTCCTCCGAGGACGTC	RFP:GCGGAGCTCTTAGG CGCCGGTGGAGTGGC
Pro2.8Kb:MOS7:GUS	Promoter: GTCGACGACACGTGATG CTCTCGTGAGC	Promoter: GCGCAGAGATAATCGGT GAAG
	cMOS7:CCCCTCGAGTGA AGAAAGTATGAAATTT AACTTTAACGAGAC	cMOS7:GGATCCCCGCCAC CGCCTCCACCCATGAAAC TGCTTTCTTGCG
Pro2.0Kb:MOS7-N	ATCCTCTAGAGTCGACC CTCATTTTCAACATTG AGA	TCGCCTGCAGGTCGACCT ACTGTAAAGCCAGTGAT GCGT
ProCYCB1;1:CYCB1;1:GFP	GTCGACCCTCGAGAGAT GACTAAATTTG	GGATCCACCTCCTCCACC GCCCTTCTCTCGAGCAGC AACTAAAC
pGBKT7:MOS7	CCCGGATCCGTAAATTT AACTTTAACGAG	CCCCTCGAGCTACCCATA CATATTAGCATC
pGBKT7:MOS7-N	CCCGGATCCGGATGAAA ACTTGGGATCTCTTG	CCCCTCGAGCTACATGAA ACTGCTTTCTTG
pGBKT7:MOS7-C	CCCGGATCCGGATGAAA ACTTGGGATCTCTTG	CCCCTCGAGCTACATGAA ACTGCTTTCTTG
pGADT7:MAD2	GGGATCGATGGATGGCG TCCAAAACAGCGGC	GGGCTCGAGTTACTCTT CTTCATCCCACTC
pGADT7:BUB3.1	GGGATCGATGGATGACG ACTGTGACTCCGTC	GGGCTCGAGCTACGCCGC AGGATTCGGGT
pGADT7:BubR1	GGGATCGATGGATGGCA GCCGAAACGAAGGTTC	GGGCTCGAGTCATCGTA GGAAGCTGTTGG
pGADT7:CDC20.1	GGGATCGATGGATGGA TGCAGGTATGAACAAC	GGGCTCGAGTCAACGAA TACGATTCACGTG
pGADT7:Rae1	GGGGAATTCATGGCAAC	GGGCTCGAGTCATTTTC

	TTTTGGTGCGCC	TGCCGGTTGCTC
pGADT7:FZR2	GAGCCCGGGCATGGAAG AAGAAGATCCTAC	GGGCTCGAGTCACCGAA TTGTTGTTCTAC
pGADT7:Nup98a	GGGCCCGGGGATGTTTG GCTCATCTAATCC	GGGATCGATCTAAACTC CATCTTCTTCATC
pGADT7:APC2	GCGGAATTCATGGAAGC TTTAGGTTCCTC	GCGGGATCCCTACTTCT TTAGCAAATACATACC
pGADT7:APC6	GGAGGCCAGTGAATTCA TGAGGGAAGAAGAAAT TGAG	CGAGCTCGATGGATCCCT AGCAGAGCTCAACCTTT G
pGADT7:APC8	CCCGGGTGGGCATCGAT GCATGGTCTCTAAAGA GTGTTG	CGAGCTCGATGGATCCCT AAATAGGAAAATGCTCG AGATC
pGADT7:APC10	GCGGAATTCATGGCGAC AGAGTCATCGGA	GCGGGATCCTCATCTCAG TGTTGAATAAG
pGADT7:Dynein	From PANBIONET corporation	
pGADT7:Kinectin		
pGADT7:Nup62	GGGCCCGGGGATGTCGG GGTTTCCATTTGG	GGGCTCGAGTCAAGACA TCCAGTGCTTTG
CaMV:nEYFP:MOS7	GCGCTCGAGCGATGAAA TTTAACTTTAACGAG	GCGGGATCCCTACATGA AACTGCTTTCTTGCGAT
CaMV:cEYFP:MOS7	GCGCTCGAGCGATGAAA TTTAACTTTAACGAG	GCGGGATCCCTACATGA AACTGCTTTCTTGCGAT
CaMV:nEYFP:Dynein	GCGGAATTCGATGAGT GACGGGAGGAGGAAG	GCGGGATCCTTAACCCGA CTTGAAGAGCAG
CaMV:cEYFP:Dynein	GCGGAATTCGATGAGT GACGGGAGGAGGAAG	GCGGGATCCTTAACCCGA CTTGAAGAGCAG
CaMV:nEYFP:Kinectin	GCGGAATTCGATGGCTG GTAAAGAGGAGAC	GCGGGATCCTCATATGT TTGATGCACTCA
CaMV:cEYFP:Kinectin	GCGGAATTCGATGGCTG GTAAAGAGGAGAC	GCGGGATCCTCATATGT TTGATGCACTCA
CaMV:nEYFP:TUA	GGACTCAGATCTCGAGG CATGAGAGAGTGCATT TCGAT	CCGCGGTACCGTCGACTT AGTATTCCTCTCCTTCA TC

3. RESULTS

3.1 Isolation of the *mos7-5* mutant showing seed set distortion

To acquire the mutants showing defective in reproductive stage of *Arabidopsis*, I acquired about 80,000 T-DNA activation tagging mutant lines. The T-DNA activation vector not only activates flanking sequences but also inactivates inserted genes (Weigel et al., 2000). The 80,000 lines were screened for seed set distortion with approximately 50% abortion, and the *mos7*-5 heterozygous mutant showing aborted ovules and aborted seeds was identified (Figure 1A). To identify the flanking sequence of T-DNA, thermal asymmetric interlaced PCR (TAIL-PCR) was performed (Liu et al., 1995). Molecular evidence showed that the T-DNA inserted into the 3rd exon of *MOS7/Nup88* (*Modifier Of Snc1,7*) (Figure 1B).

To observe the phenotypes, pistils of FG7 stage and siliques (DAP 1 to 8) were dissected, and ovules and seeds were mounted in clearing solution. Ovules that contained only a single nucleus or bi- nuclei were detected in a *mos7*-5 heterozygous mutant, indicating that development of embryo sacs was impaired (Figure 1C). Alexander staining of pollen grains which can distinguish

between the functional viable and aborting pollen showed many pollen were aborted before fertilization (Figure 1D). These results suggest that MOS7 has a critical role in both gametophytes development in *Arabidopsis*. After fertilization, embryo lethal phenotype was also observed in a developing silique of the *mos7-5* heterozygous mutants. Abnormality in the *mos7-5* mutant embryos was first detected at the globular stage (Figure 2). These results showed that MOS7 is involved in whole reproductive stage in *Arabidopsis* including gamete formation and seed development.

Figure 1

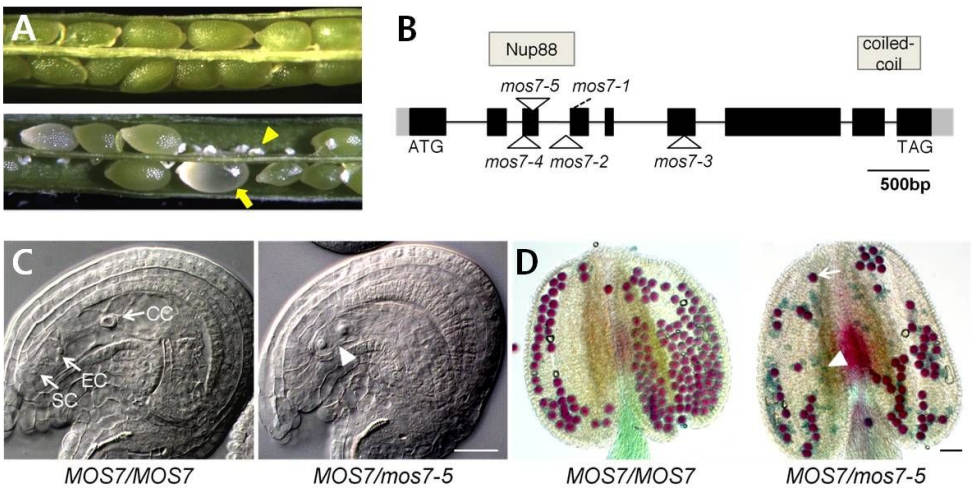

Figure 1. Isolation of *mos7-5* showing defects in reproductive stage

(A) Open siliques from wild-type (upper panel) and *mos7-5* (lower panel) plants. Arrowhead indicates aborted ovules and arrow indicate seed abortion.

(B) Schematic diagram showing structure of the *MOS7* gene with T-DNA flanking region of several mutant alleles. Black box, translated exon; gray box, untranslated exon; line, intron. The insertion sites of T-DNAs are marked by triangles.

(C) Wild-type ovule and a mutant ovule in *MOS7/mos7-5* plants before fertilization. Arrowhead indicates an arrested two-nucleated embryo sac.

(D) Alexander staining of a wild-type stamen and a *MOS7/mos7-5*

stamen. Red stained pollen grains are viable (arrow) and green shrunken ones (arrowhead) are non-viable. SC, synergid cell; EC, egg cell; CC, central cell. Scale bars = 25 μm (C and D)

Figure 2

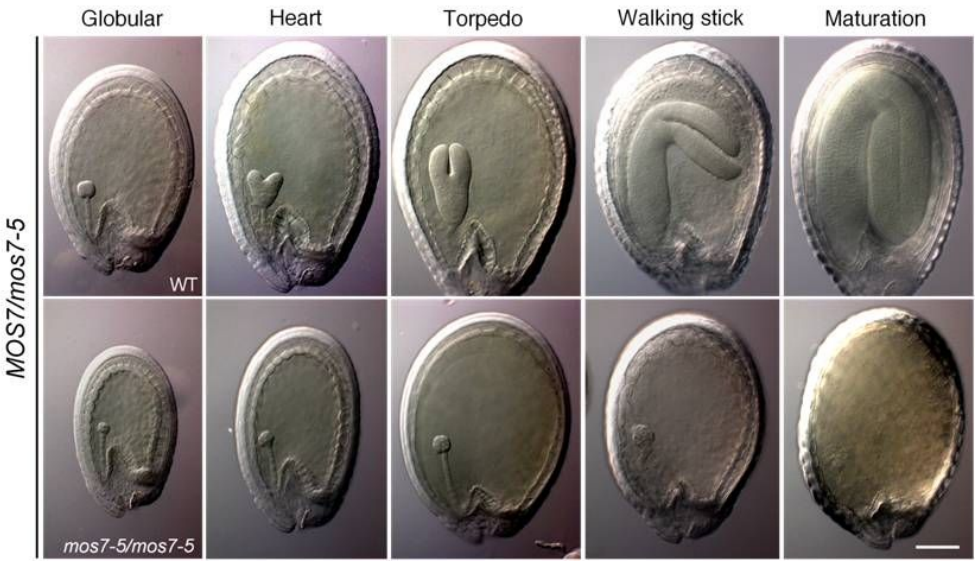

Figure 2. Embryonic lethal phenotype of *MOS7/mos7-5*

Representing images were shown in *MOS7/mos7-5* heterozygous plants; normal embryogenesis (upper panel), or delayed and arrested embryogenesis (lower panel). Scale bar = 100 μm

3.2 Molecular cloning of the *MOS7* gene

Before the characterization of *mos7-5* allele, five times back crosses were performed, because multi-copies of T-DNA in chromosomal regions may possibly cause an unintended defect. The multiple backcross and reselection procedure enable a mutant line to show monogenic inheritance.

To examine whether the *mos7-5* mutant is a knockout allele, I used reverse transcription (RT)-PCR and quantitative RT (qRT)-PCR to check the alteration of MOS7 expression in floral buds. As described above, *mos7-5* T-DNA inserted into 3rd exon of *MOS7* on chromosome 5. I obtained three additional other mutant alleles, *mos7-2 (Salk_129301), mos7-3 (Salk_085349)* and *mos7-4 (CS822857)* from ABRC, Ohio State University (Figure 1B). Through both RT-PCR analyses, it was identified that *MOS7* transcripts were significantly reduced in the floral buds of *mos7-2, mos7-3 and mos7-5* heterozygous mutants when using the primer set to detect the last exon (Figure 3, A and B). When the primer set for the 4th exon was used, *mos7-2* and *mos7-5* heterozygous mutants, but not *mos7-3* heterozygous mutants, showed significant reduction of the transcripts due to the T-DNA insertional sites in *MOS7* gene (Figure 3, A and B).

To examine whether the over-expression was induced by the T-DNA in *mos7-5* mutant, I used quantitative RT-PCR to check the alteration of genes flanking the T-DNA in floral buds. However, no significant ectopic expression of *MOS7*-nearby genes was observed, indicating that *mos7-5* is a recessive loss-of-function mutation (Figure 3C). No homozygous mutants were obtained in any of the mutant lines, further confirming that *mos7-2, mos7-3* and *mos7-5* are recessive alleles.

To confirm that ovule and seed abortion phenotype was caused by the insertional mutation in *MOS7*, I transformed the MOS7 transgene under the control of the own promoter (*Pro2.0kb:MOS7:GFP*) into *MOS7/mos7-5* heterozygous plants. The complementation test showed that ovule/seed set distortion in the *mos7-5* mutant was rescued by introducing functional *MOS7* gDNA (Table 3). These results showed that the phenotype was correlated with the MOS7 mutation and MOS7 expression is required for gamete and seed viability in *Arabidopsis*.

Figure 3

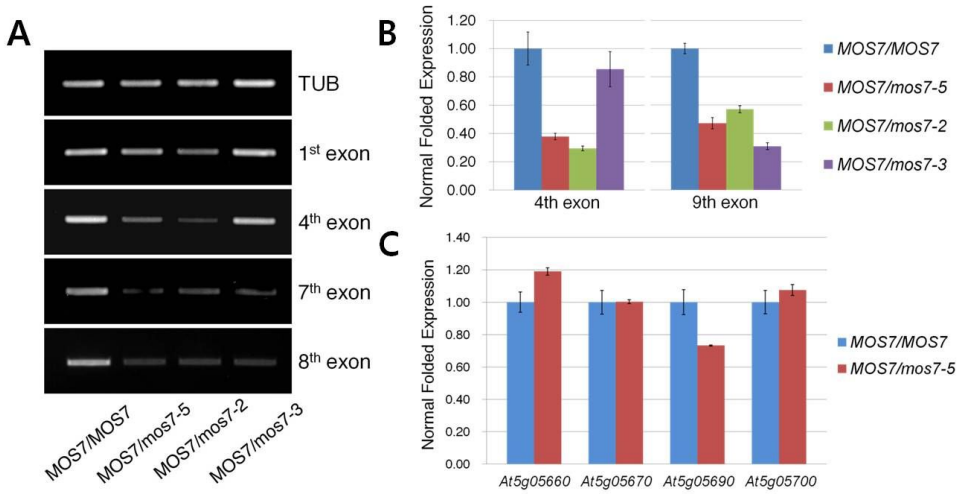

Figure 3. Molecular cloning of the *MOS7* gene

RT-PCR (A) and quantitative RT-PCR (B) analysis was performed to check the expression of *MOS7* and *MOS7*-nearby genes (C) using gene specific primers. Total RNA was extracted from floral buds (flowering stages 1-10) of wild-type, *MOS7/mos7-5*, *MOS7/mos7-2* and *MOS7-3* mutant. Transcript levels were normalized with *TUB* levels. *At5g05660,* Encode a homolog of the mammalian zinc finger transcription factor NF-X1; *At5g05670,* Function in signal recognition particle binding; *At5g05690,* Encodes a member of the CP90A family; *At5g05700,* Encodes an arginyl-

tRNA:protein transferase (ATE1). Error bars indicate the SEM of three PCR replicates.

Table 3

Parental Genotypes (female x male)	Percentage of Seeds			Total (n)	$\chi 2$	P
	Normal Seed (%)	Seed Abortion (%)	Ovule Abortion (%)			
Col-0 x *Col-0*	99.4	0.0	0.6	663		
MOS7/mos7-5 x *MOS7/mos7-5*[a]	38.9	13.5	47.6	1680	4.2917	0.1170[b]
MOS7/mos7-2 x *MOS7/mos7-2*[a]	46.1	7.7	46.2	1436	45.0028	<0.0001[b]
MOS7/mos7-4 x *MOS7/mos7-4*[a]	40.1	11.5	48.4	1829	5.5482	0.0624[b]
MOS7/mos7-3 x *MOS7/mos7-3*	70.6	23.7	5.7	493	1.5963	0.2064[c]
MOS7/mos7-5 x *Col-0*	51.0	0.2	48.8	820		
Col-0 x *MOS7/mos7-5*[a]	95.5	1.1	3.4	375		
MOS7/mos7-3 x *Col-0*	97.6	0.0	2.4	127		
Pro2.0kb:MOS7:GFP/Pro2.0kb:MOS7:GFP in mos7-5/mos7-5	99.1	0.0	0.9	583		
Pro2.8kb:cMOS7:GUS/Pro2.8kb:cMOS7:GUS in mos7-5/mos7-5	92.9	0.1	7.0	1405		

Table 3. Analysis of seed viability and complementation

Abortion ratio = (No. of aborted seeds or ovules/No. of total seeds) × 100%.

a: Much pollen abortion was discovered when used for pollen donor.

b: Probability that deviation from a 3:1:4 segregation of normal

seeds, aborted seeds, and aborted ovules is due to chance. Since half of the meiotic products carrying over the MOS7 product will survive, and the other half will be dead regardless of the *mos7-5* haploid genotype *per se,* I expect 4 (survived):4 (dead) before fertilization. After fertilization among four survived, 3(viable):1 (aborted) seeds are expected.

c: Probability that deviation from a 3:1 segregation of viable and aborted seeds is due to chance.

3.3 Phenotypic analysis of ovules in the *mos7-5* mutant

As described above, *mos7-5* mutants show abnormal ovules with a single nucleus or bi- nuclei before fertilization. To characterize cell identity in arrested embryo sac, I introduced cell-specific markers into *mos7-5* heterozygous mutants using the following genetic crosses: *DD1:GFP* (antipodal cell), *DD2:GFP* (synergid cell), *DD45:GFP* (egg cell), and *DD7: GFP* (central cell) (Steffen et al., 2007). Although a strong GFP signal was detected in half of the ovules of *mos7-5* heterozygous mutants, none of the arrested ovules showed GFP expression (Figure 4A to 4D). In contrast, when I introduced *FM2:GUS*, a functional megaspore (FM) marker (Olmedo-Monfil et al., 2010), GUS was strongly expressed in an arrested embryo sac (Figure 4E). Therefore, the cell in the arrested embryo sac has FM-like identity. This result indicates that after megasporogenesis, megagametogenesis development of embryo sac was perturbed.

I confirmed again by confocal microscopy that defective ovules in the *mos7-5* mutants were arrested after FG1 stage. Consistent with the GUS data, no discernible differences were observed during meiotic division in the ovules of *MOS7/mos7* (Figure 5A). However,

about 50% of the defective ovules in the *MOS7/mos7* mutants showed strong autofluorescent mass, the degenerating megaspores before the first mitotic division (Figure 5B, arrowheads). Subsequent mitotic divisions were not completely processed, resulting in either a single nucleus or two nuclei inside the embryo sac (Figure 5B). Even though defective ovule proceeds to bi-cellular stage occasionally, the two nuclei did not move away from each other, nor was a large central vacuole observed. These results indicate that megagametogenesis did not proceed beyond the FG2 stage and that the development of embryo sacs was impaired.

Figure 4

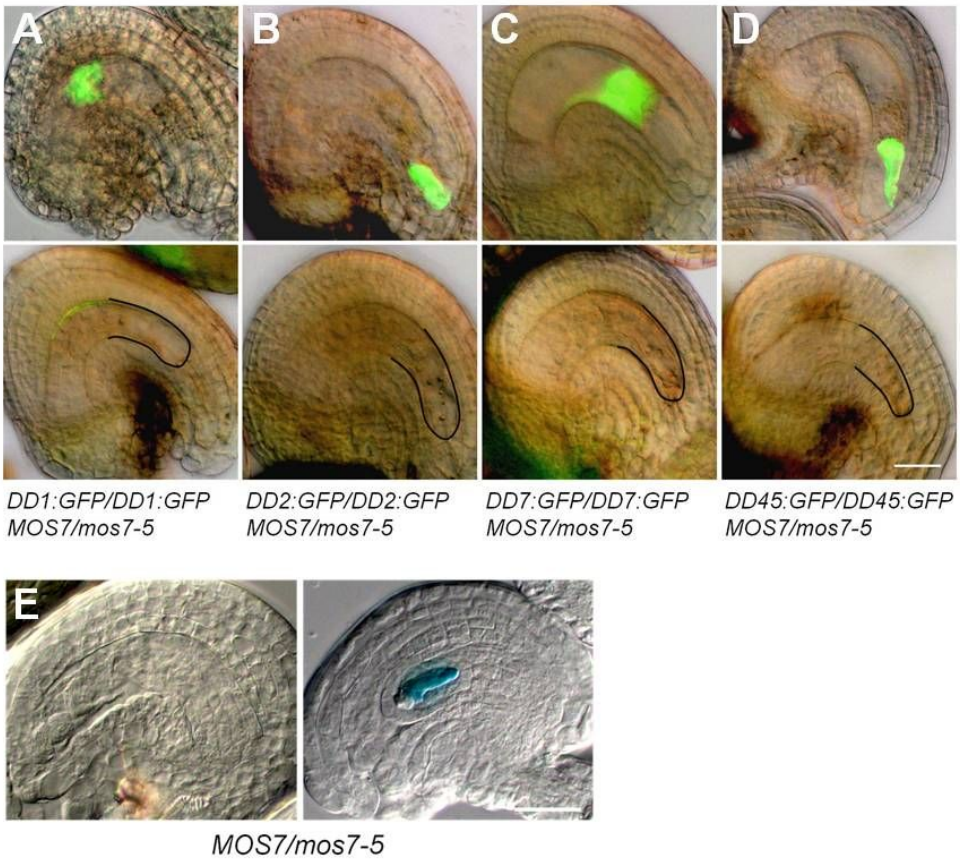

Figure 4. FM-like cell identity of the arrested cells in the *mos7-5* mutant ovules

(A to D) The series of gametophytic cell maker were introduced into the *MOS7/mos7-5* plants. From the same pistil, normal ovules showed strong GFP expression (upper panel), and the other showed no expression (lower panel) in an embryo sac.

(A) *DD1:GFP/DD1:GFP MOS7/mos7-5* (antipodal cell).

(B) *DD2:GFP/DD2:GFP MOS7/mos7-5* (synergid cell).

(C) *DD7:GFP/DD7:GFP MOS7/mos7-5* (central cell).

(D) *DD45:GFP/DD45:GFP MOS7/mos7-5* (egg cell).

(E) A functional megaspore marker, *FM2:GUS*, is not expressed in normal ovule at mature stage (FG7), but is expressed in an arrested ovule of the same pistil in a *FM2:GUS/FM2:GUS MOS7/mos7-5* plant.

(A to D)Images are created by merging a DIC image with a GFP image. Scale bars = 25 μm.

Figure 5

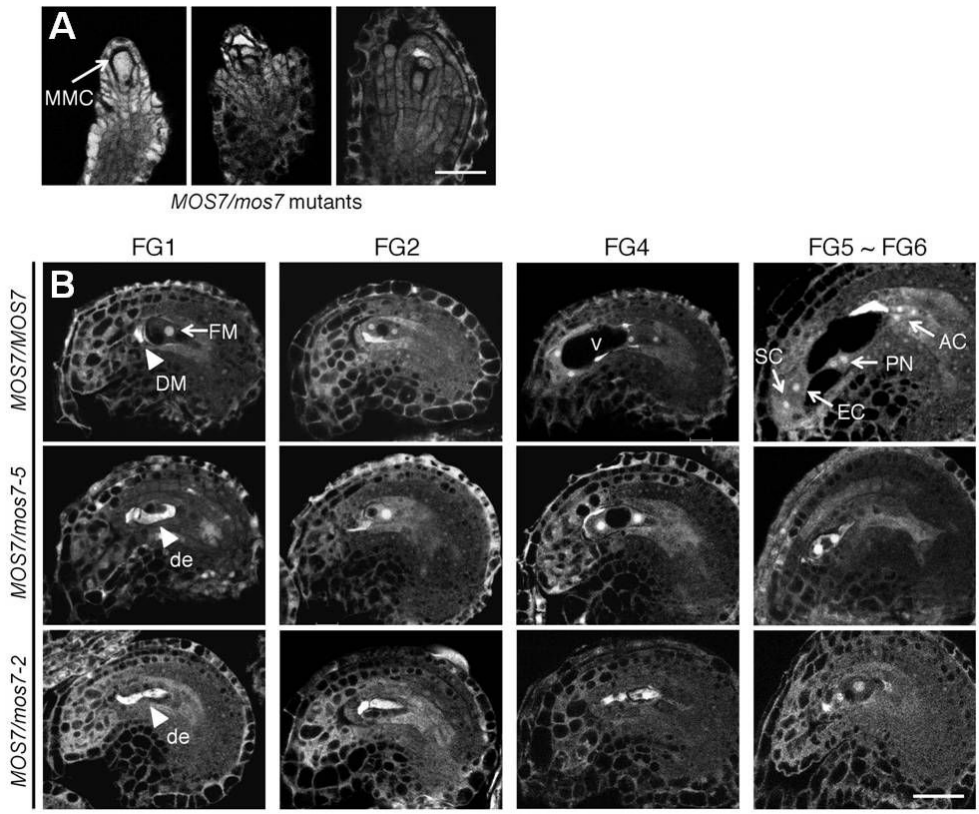

Figure 5. CLSM images of female gametophytes in *mos7-5* mutant

(A) Meiotic division from a diploid MMC (arrow) to FG1 stage ovule of a *MOS7/mos7-5* plant. No defects were observed during meiosis. (B) Wild-type (top), *MOS7/mos7-5* (middle), and *MOS7/mos7-2* (bottom) ovules at the same growth period. A wild-type ovule in FG1 stage showed meiotic products, FM (arrow) and DM (arrowhead). Three mitotic divisions from FM occurred, and an

eight-nucleated embryo sac was observed (FG5 stage). *MOS7/mos7-5* and *MOS7/mos7-2* ovules displayed abnormal FG1 embryo sacs followed by failure of successive mitotic divisions. Degenerated nuclei (arrowhead) were visualized by their strong autofluorescence.

MMC, megaspore mother cell; DM, degenerated megaspore; FM, functional megaspore; de, degenerated embryo sac; V, vacuole; SC, synergid cell; EC, egg cell; PN, pollar nucleus; AC, antipodal cell. Cytoplasm is displayed as gray, vacuoles as black, and nucleoli as white. Scale bars = 25 μm.

3.4 Phenotypic analysis of pollen in the *mos7-5* mutant

As described in Figure 1D, from the analysis of pollen viability using Alexander staining, I suspected that mitotic defect leading to pollen abortion occurred in *mos7-5* mutants. To visualize mitotic defects during microgametogenesis in *mos7-5*, the *ProHTR12:HTR12:GFP* transgene, a centromere marker (Talbert et al., 2002; Fang and Spector, 2005; Ingouff et al., 2007), was introduced into the *mos7-5* mutant by genetic cross. Because *HTR12* encodes a centromeric histone H3 variant, chromosome segregation during pollen development could be observed. HTR12:GFP was expressed at all five chromosomal centromeres in wild-type microspores and in the subsequent generative cell and vegetative cell during PMI (Figure 6A).Thereafter, GFP was no longer detected in the vegetative cell nucleus. Only the generative cell and subsequent sperm cells showed HTR12:GFP expression, consistent with Chen et al. (2009) (Figure 6, C and D). All microspores from the heterozygous *mos7-5* mutant showed a similar expression pattern to that of the wild-type microspores (Figure 6E). However, strong yet diffuse GFP fluorescence with occasionally localized expression was observed in morphologically

irregular nuclear structures during PMI (Figure 6F). Although most of the defective pollen arrested during PMI stage, some abnormal division occurred occasionally although the mutants never showed a normal, discrete HTR12:GFP expression (Figure 6G). Perhaps CenH3 was no longer incorporated normally or was not stable in the mutant chromosome during microgametogenesis.

In total, these results demonstrated that mutations in *MOS7* caused mitotic defects during female and male gametogenesis in *Arabidopsis*.

Figure 6

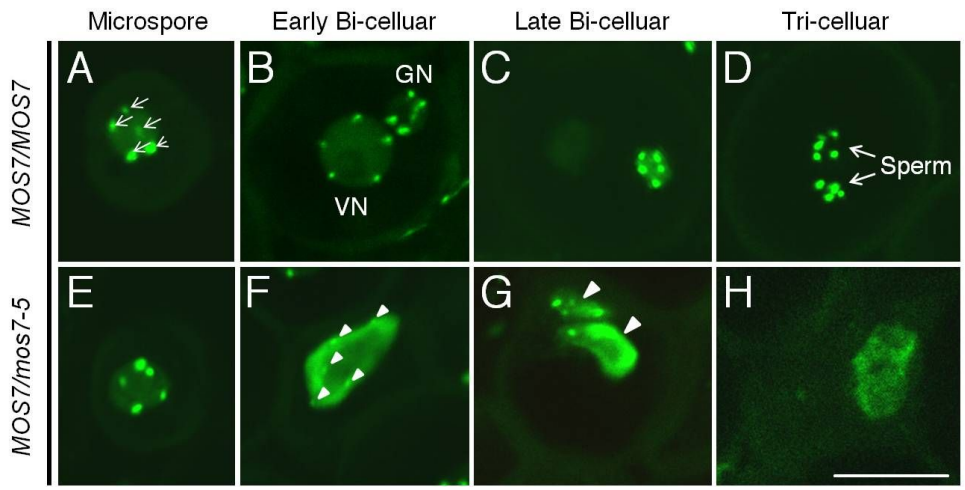

Figure 6. Phenotypic analysis of male gametes in *mos7-5* mutant

A-H, HTR12:GFP protein was observed as bright dots at the centromeres. Developing pollen grains from wild-type (A-D) were photographed using confocal microscopy at the same growth period as *MOS7/mos7-5* mutant pollen grains (E-H).

A, Microspore with five centromeres (arrow).

B, Early bi-cellular stage after PMI with GFP expression both in generative cell and vegetative cell.

C, Late bi-cellular stage with GFP expression only in generative cell.

D, Tri-cellular stage after PMII with GFP expression in two sperms (arrows).

E–H, Abnormal mitotic divisions of the developing pollen grains in *MOS7/mos7–5* plants.

F, Defect in karyokinesis with diffused GFP signals.

G, Defect in cytokinesis with abnormal nuclear structure.

H, Shrunken pollen grain. Scale bar = 10 μm.

3.5 MOS7 N-terminal domain is implicated in gametophytic development

In self-pollinated heterozygous *MOS7/mos7-5* plants, I counted an abortion ratio and found that 48% of the total ovules aborted and 14% of the seeds aborted (n=1,680). The *mos7-2* mutant also showed a similar ratio of gametophytic and zygotic lethal phenotype as that of *mos7-5* mutants (Table 3). However, the *mos7-3* heterozygous mutant showed only 24 % zygotic lethal (n=493), with rare gametophytic lethality in the developing siliques, suggesting that *mos7-3* mutant follows simple Mendelian inheritance (X^2 = 1.5963 for the 3:1 ratio, P > 0.2; Table 3).

Since *mos7-3* T-DNA is inserted into the 6^{th} exon, which is closer to the C-terminal region of MOS7 than the insertion locations of *mos7-2* or *mos7-5*, the truncated MOS7 N-terminal protein produced in *mos7-3* plants, but not in *mos7-2* or *mos7-5* plants. Truncated partial protein might be responsible for successful female and male gametogenesis. To explore this possibility, the *mos7-5* mutant plants were directly transformed with a transgene containing the MOS7 N-terminal region (Figure 16A, see below) and looked for the gametophytic complementation. However, there was no reduction of the gametophytic ovule abortion ratio when I

counted the abortion ratio of the F1 plants (*MOS7/mos7-5*; hemizygous for *Pro2.0kb:MOS7-N*). Rather, the ovule abortion ratio was higher than that of *mos7-5* plants (Figure 7). Moreover, the abortion ratio was proportional to the expression level of the transgene MOS7 N-terminal domain. It is possible that the dominant negative N-terminal MOS7 domain sequesters other binding factors that are required for normal MOS7 function. Consistent with this idea, Hashizuma et al. (2010) reported that both over-expression and knock-down of human Nup88 induced multinucleated cells leading to cancer. Therefore, a proper expression of the MOS7 N-terminal region is critical for gametogenesis. Also, MOS7 N-terminal over-expression in a wild-type background caused variation in the ovule abortion ratio, depending on the plant line, further supporting the idea that balanced *MOS7* expression is important for accomplishing gametogenesis (Figure 8).

Figure 7.

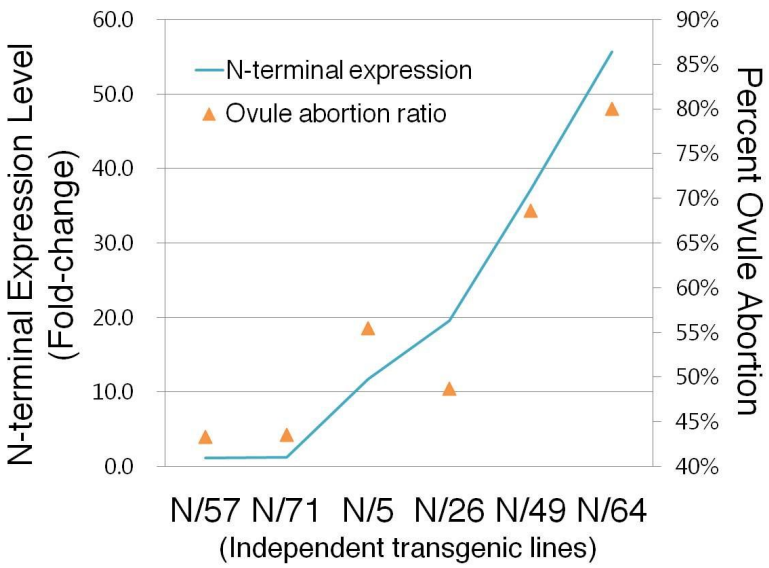

Figure 7. Critical function of the N-terminus of MOS7 on gametogenesis

Expression of the MOS7 N-terminus was measured in several independent transgenic lines (X axis). The change in transcription of the 4th exon of *MOS7* was measured using quantitative RT-PCR and the fold changes in expression were calculated (Left-hand Y axis; solid line). These values were plotted against the percentage of ovule abortion observed respectively in each transgenic line (Right-hand Y axis; triangles).

Figure 8

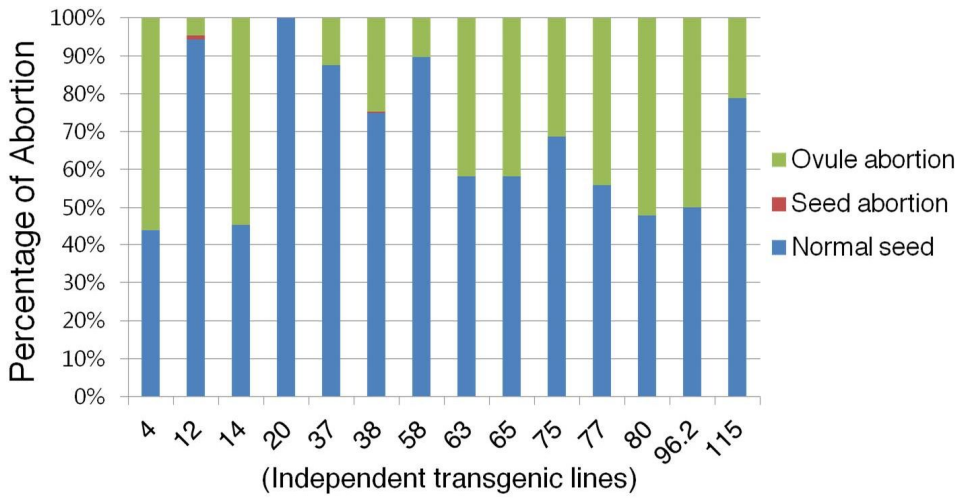

Figure 8. Critical function of N-terminal of MOS7 on gametogenesis in wild-type background

In a wild-type background, *MOS7* N-terminal over-expression caused variation in the ovule abortion ratio depending on the plant line.

3.6 MOS7 C-terminal domain is implicated in zygotic development

As described previously, in self-pollinated heterozygous *MOS7/mos7-3* plant, I counted seed abortion and found that the mutant showed only 24 % zygotic lethal (n=493), with rare gametophytic lethality in the developing siliques, following simple Mendelian inheritance (Table 3). Since the insertion location of *mos7-3* T-DNA is closer to the C-terminal region than the other alleles, it is possible that the truncated MOS7 N-terminal protein produced in *mos7-3* plants might be responsible for successful female and male gametogenesis. To explore this possibility, quantitative RT-PCR was performed using primer set for the 4th exon. The result shows that the transcription level of *MOS7* gene in *mos7-3* plants was similar to that of the wild-type, but significantly reduced in the floral buds of *mos7-2* and *mos7-5* heterozygous mutants (Figure 3, A and B).

I confirmed by quantitative RT-PCR that aborted seeds in the *mos7-5* mutants were homozygous (Figure 9). Seed abortion in *mos7-5* was complemented when the entire *MOS7* region including the C-terminal domain was introduced (Table 3), suggesting that the MOS7 C-terminal region is likely responsible for zygotic

embryogenesis, at least in part. In the yeast two hybrid (Y2H) screen, I identified another nucleoporin protein, Nup62, as a MOS7-interacting partner (Figure 20A, see below). The MOS7 interaction with Nup62 was through the MOS7 C-terminal region, not the N-terminal region. Interestingly, the *nup62* mutant was identified as an emb2766 mutant that showed zygotic seed abortion similar to the *mos7-3* mutant at the globular stage (http://seedgenes.org/GeneList,*Nup62/EMB2766*;*MOS7/EMB2789*; Figure 10). Thus, it is possible that the MOS7 C-terminal domain interaction with Nup62 is required for zygotic seed development after fertilization. Overall, it is likely that the MOS7 N-terminal and C-terminal region contribute to gametogenesis and post-embryonic development, respectively.

Figure 9

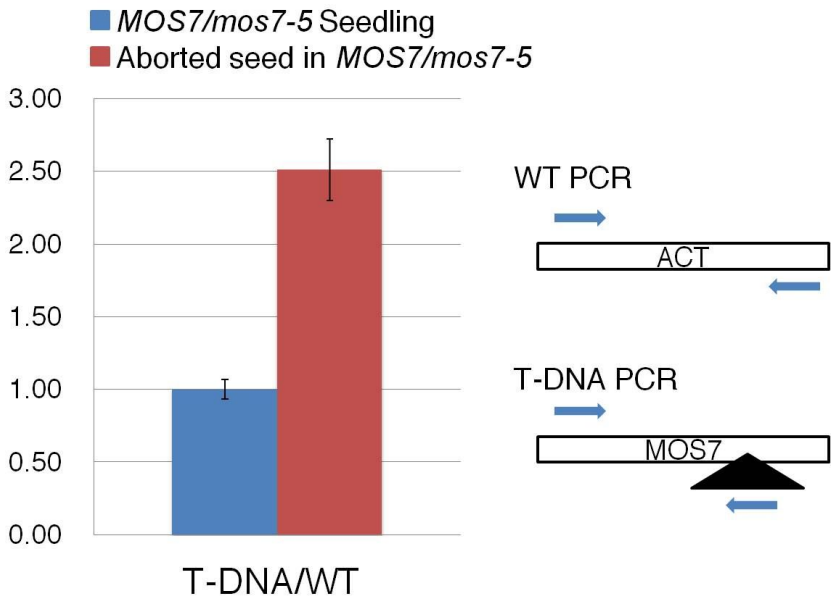

Figure 9. Genotyping of aborted seeds by quantitative RT-PCR

For genotyping of aborted seed in *MOS7/mos7-5* mutant, two quantitative RT-PCR analysis were performed using primer sets for 'WT PCR' and 'T-DNA PCR'. The result from *MOS7/mos7-5* seedling was used as internal control in which half of genomic DNA should carry *mos7-5* allele and the other half carry wild-type allele. In experiments using gDNA from aborted seeds, more than double amplification was estimated. Considering the fact that seed brings triploid endosperm, it was convincible and

the genotype of aborted seed is homozygote. Error bars indicate the SEM of three biological replicates

Figure 10

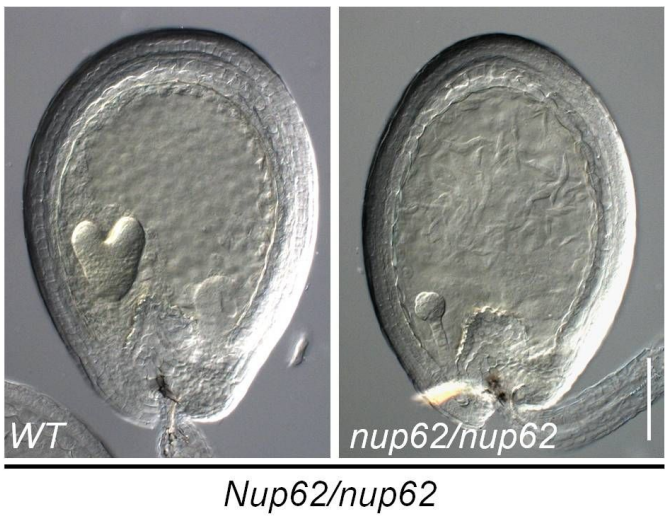

Figure 10. Developing seeds in the same silique of *Nup62/nup62*

Representing images of *Nup62/nup62* heterozygous plants showing normal embryogenesis (left) and delayed and arrested embryogenesis (right). Scale bar = 100 μm

3.7 The haplo-insufficient *mos7-5* allele in MMC and PMC results in delayed phenotypic defects after meiosis during subsequent mitotic divisions

As described above, self-fertilized heterozygous *mos7-5* plants produced 48% ovule abortion and 14% seed abortion (Table 3; n=1,680), with much pollen abortion (Figure 1D). Additionally, I pollinated heterozygous *mos7-5* female plants with wild-type pollen and observed that 49% of the ovules were aborted prior to fertilization (n=820). Given that heterozygote females produce ovules in a ratio of 1 *MOS7* : 1 *mos7-5*, a likely hypothesis was that all of the aborted ovules were of the *mos7-5* genotype. Therefore, when crossing a mutant female plant with wild-type pollen, I expected all surviving progeny to be *MOS7/MOS7*. Surprisingly, 45% of the surviving progeny (n=244) were *mos7-5* heterozygous plants (Table 4). In fact, the transmission efficiency of the *mos7-5* allele was 82.1%, not statistically different than that expected from the normal hybrid x wild-type cross (χ^2=2.361, p=0.1244, df=1). Consequently, some of the aborted ovules must have been *MOS7*, and some of the surviving ovules must have been *mos7-5*.

Many pollen grains were aborted in the self-crosses involving

the *mos7-5* heterozygous mutants (Figure 11, B and C). As with the ovule data, I initially hypothesized that the *mos7-5* mutation accounted for the aborted pollen. When wild-type plants were pollinated with *mos7-5* heterozygous pollen donors, many pollen grains did die before fertilization. However, 44% of the progeny were *mos7-5* heterozygous mutants (n=752) (Table 4). The transmission efficiency of 77.4% indicates that the *mos7-5* allele is clearly being transmitted to the next generation, although at a significantly lower ratio than normal (χ^2=12.255, p=0.0019, df=1). For the *mos7-5* allele to be transmitted to the progeny, some of the surviving pollen grains must have been of the *mos7-5* genotype.

Based on these reciprocal crosses and transmission analysis of the *mos7-5* allele, the haploid genotype does not solely determine survival of the ovule and pollen grain. Both wild-type and *mos7-5* mutants were found among the aborted and among the surviving gametophytes. To further explore this hypothesis, I generated plants that were homozygous for the quartet (*qrt*) mutant and heterozygous for the *mos7-5* mutant (*qrt/qrt MOS7/mos7-5*). Quartet mutants produce tetrad pollen due to the failure of microspore separation (>95%; Figure 11A). *qrt* mutant pollen is released in the tetrads that are viable and fertile (Preuss et al., 1994). Of the total *qrt* pollen (n=2093), 73 % exhibited two pollen

grains viable and two pollen grains dead (Figure 11, A, B, and C, 2). I also observed significant numbers of *qrt* pollen that were either all viable (21 %, 4) or all dead (4 %, 0) (Figure 11, A, B, and C). If incomplete penetrance is to fully explain the seeming contradiction between the high abortion ratio and high *mos7-5* transmission, there should be a high percentage of *mos7-5* haploid pollen in viable tetrad pollen. Accordingly, I collected only the viable pollen grains from 4-, 3-, 2-, and 1-*qrt* tetrads (Figure 11A) after manually removing any aborted pollen, and checked the genotype of the viable pollen. The result shows while the wild-type allele displayed 100% transmission ratio, the transmission of the mutant *mos7-5* allele accounted for 72% in the total viable pollen grains (Figure 12). A reduction from the normal ratio that is marginally significant (t-test, t=2.1574, p=0.0972, df=4). The mutant *mos7-5* allele was detected in about 42% and the wild type allele was detected in about 58% of the total viable pollen grains. The reduced detection of *mos7-5* allele in the genomic DNA PCR versus the expected 50:50 segregation ratio was statistically significant (one sample t-test, t=5.5944, p=0.0305, df=2). This result suggests that the *mos7-5* allele causes gametophytic defects. It also explains the 77.4% transmission efficiency of the *mos7-5* allele when hybrid males are crossed with wild-type females (see Table 4). In general,

not all segregating *mos7-5* mutant pollen is dead and, conversely, not all segregating wild-type pollen is viable. Based on the analysis, in the haploid microspore, inheriting the *mos7-5* mutant allele from the diploid PMC does not co-segregate with the abortion phenotype. One possible explanation is that the *mos7-5* allele is haplo-insufficient in diploid MMC and PMC so that it produces half of the amount of *MOS7* RNA or protein that will be required later during gametogenesis. During subsequent mitotic divisions, half of the meiotic products carrying over the MOS7 product will survive, and the other half will be dead regardless of the *mos7-5* haploid genotype *per se*.

Indeed, *MOS7:GFP* starts to be expressed in the 2n MMC and PMC during reproduction (Figure 15, H, I, and M, see below). Hypothesis for MOS7-carrying over from maternal tissue will be discussed in the discussion section. These data support the idea that MOS7 is also required in diploid MMC and PMC before meiosis, and during meiosis.

Figure 11

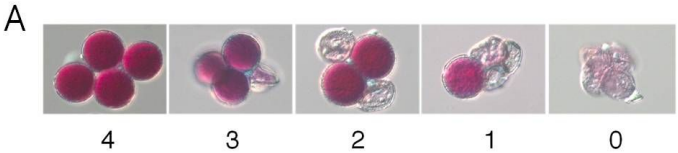

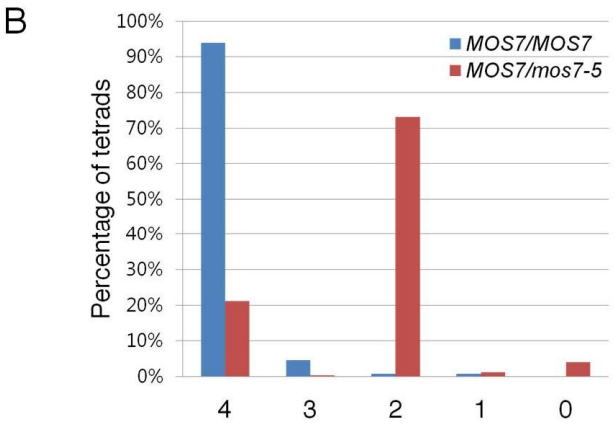

C

Tetrad number	4	3	2	1	0
MOS7/MOS7 (percentage)	124 (93.9)	6 (4.5)	1 (0.7)	1 (0.7)	0 (0)
MOS7/mos7	443 (21.2)	9 (0.4)	1531 (73.1)	25 (1.2)	85 (4.1)

Figure 11. Transmission analysis of *mos7-5* mutant allele using *qrt/qrt MOS7/mos7-5* mutants

A, DIC images of Alexander staining of the *MOS7/mos7-5* pollen in a *qrt/qrt* background. [4], a tetrad of four normal pollen grains; [3], a tetrad of three viable and one aborted; [2], a tetrad of two viable and two aborted; [1], a tetrad of one viable and three aborted; [0], a tetrad with all aborted tetrad.

B and C, Percentage of tetrads containing 4, 3, 2, 1 or 0 normal pollen grains in wild-type versus the *MOS7/mos7-5* mutant.

Figure 12

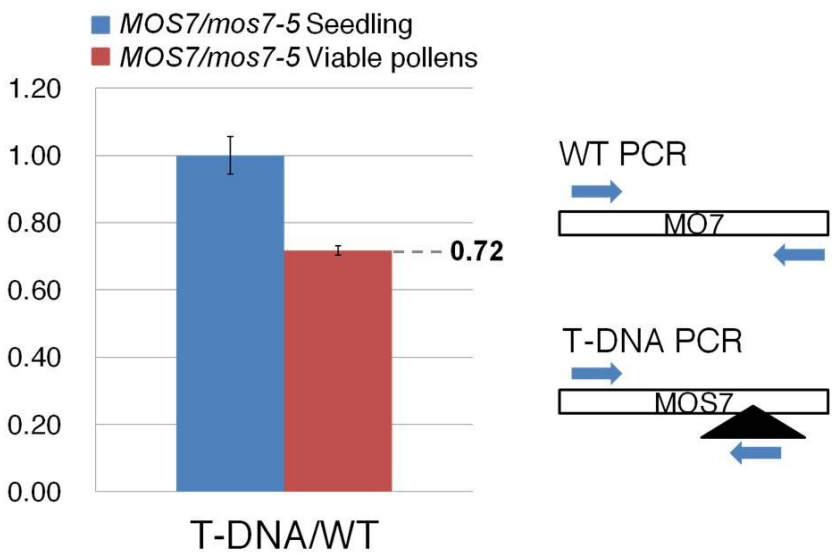

Figure12. Transmission efficiency assay of *mos7-5* allele

Two quantitative RT-PCR analyses were performed using primer sets for 'WT PCR' and 'T-DNA PCR'. The result from a *MOS7/mos7-5* seedling was used as an internal control, as half of the genomic DNA should carry the *mos7-5* allele and the other half carry the wild-type allele. 72% transmission efficiency was confirmed using gDNA from all viable pollen grains as the template. Error bars indicate the SEM of three biological replicates.

Table 4.

Parental genotypes (female x male)	Progeny (n)			TE_F (%)	TE_M (%)
	MOS7/MOS7	*MOS7/mos7*	Total		
Col-0 x *Col-0*	395	0	395		
MOS7/mos7-5 x *Col-0*	134	110	244	82.1	
Col-0 x *MOS7/mos7-5*	424	328	752		77.4

Table 4. Transmission analysis of *mos7-5* allele

F1 seeds of the resulting cross of *mos7-5* with wild-type were collected and grown on basta containing MS plates to determine the efficiency of mutant allele transmission to the next generation through female and male gametes. Transmission efficiency; TE = (No. of progeny plants with T-DNA insertion/No. of progeny plants without T-DNA insertion) × 100%. TE_F, female transmission efficiency; TE_M, male transmission efficiency.

3.8 *MOS7* is expressed in various tissues and cells including MMC and PMC

Using RT-PCR analysis, it was confirmed that *MOS7* is expressed throughout the plant, with higher expression in inflorescences (Figure 13). To observe spatiotemporal expression, I analyzed *Pro2.8kb:cMOS:GUS* transgenic plants – with *MOS7* cDNA fused to *β-glucuronidase* (*GUS*) driven by 2.8 kb *MOS7* flanking sequences. Consistent with quantitative RT-PCR results, GUS activity was observed in various tissues such as roots, leaf primordia, cotyledons and nuclei of true leaves and trichomes (Figure 14A to 14E). During the reproductive stage, GUS activity was detected in the megaspore of FG1 stage ovules (Figure 14F).

To evaluate *MOS7* expression at the cellular level during reproduction, I generated transgenic plants expressing the MOS7:GFP fusion protein under the control of a 2.0kb *MOS7* promoter (*Pro2.0kb:MOS:GFP*). First, I confirmed that this transgenic produces functional MOS7 using a complementation test (Table 3). Then, I observed GFP fluorescence. The 2n MMC expressed GFP in the nuclear rim and partially in the cytoplasm (Figure 15A) – a pattern also observed in animal Nup88 (Griffis et

al., 2003; Hashizume et al., 2010). GFP was also detected in the subsequent functional megaspore (Figure 15B). After that stage, MOS7:GFP was observed from the FG1 to FG2 stages (Figure 15C), when the first mitotic division occurs during megagametogenesis (Christensen et al., 1997). GFP expression remains in mature female gametophytes (Figure 15D).

Similarly, MOS7:GFP was observed in the nucleus rim and the cytoplasm of the 2n PMC and of the dyad and tetrad pollen during meiosis (Figure 15, E, F, and G). GFP was continuously detected during pollen mitosis I (PMI) and II (PMII) (Figure 15, H, I, and J). After fertilization, MOS7:GFP was detected in the developing embryo, endosperm and seed coat (Figure 15K).

Overall, the MOS7:GFP localization pattern overlapped with the phenotypes that were observed in gametogenesis. These results support the hypothesis that MOS7 is required in the MMC, PMC, and during meiosis, although the phenotype is seen later during mitotic division.

Figure 13

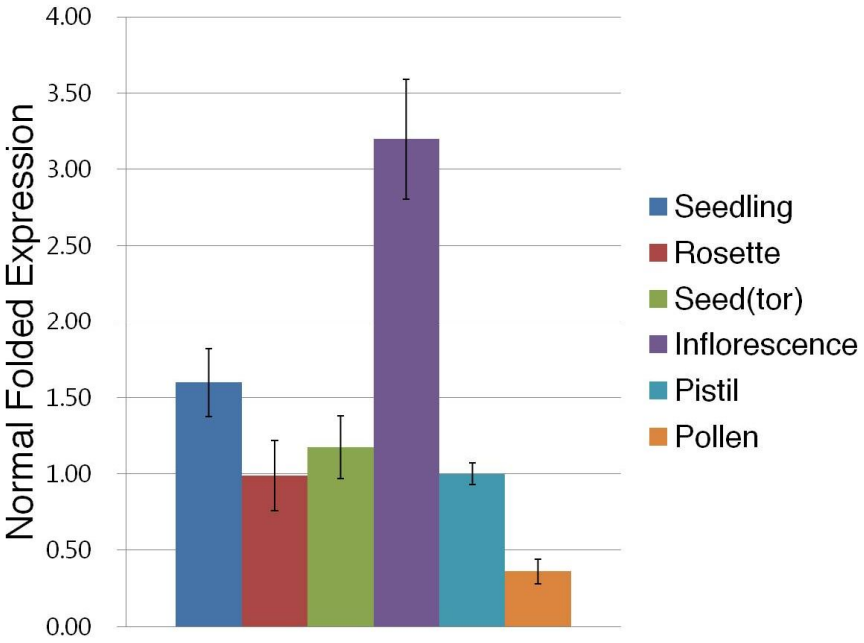

Figure 13. *MOS7* expression in various tissues and cells

Quantitative RT-PCR for *MOS7* was performed with cDNAs from seedlings (2 weeks old), rosette leaves, seeds (torpedo), inflorescences (floral stage at 1 to 13), pistils, and pollen. *MOS7* transcript levels were normalized to *TUB* levels. Error bars indicate the SEM of three biological replicates.

Figure 14

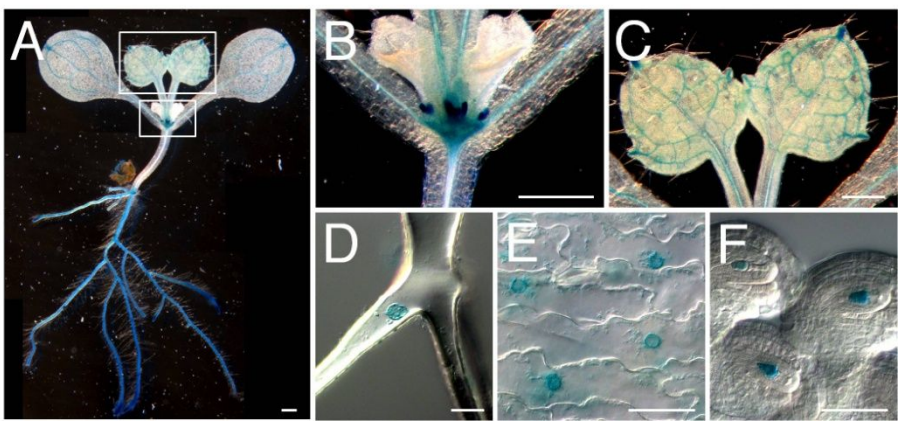

Figure 14. Representative images of the *Pro2.8kb:cMOS7:GUS* expression

A, MOS7:GUS expression in 8 days-old seedlings.

B and C, Close-up views as indicated by rectangles in (B) showing strong GUS expression at the leaf primordia and leaf veins.

D and E, MOS7:GUS localization at the nuclear rim of the trichome (D)and leaf epidermis (E).

F, Strong MOS7:GUS expression in FM of the embryo sac (FG1 stage). Scale bars = 500 μm (A-C), 50 μm (D-F).

Figure 15

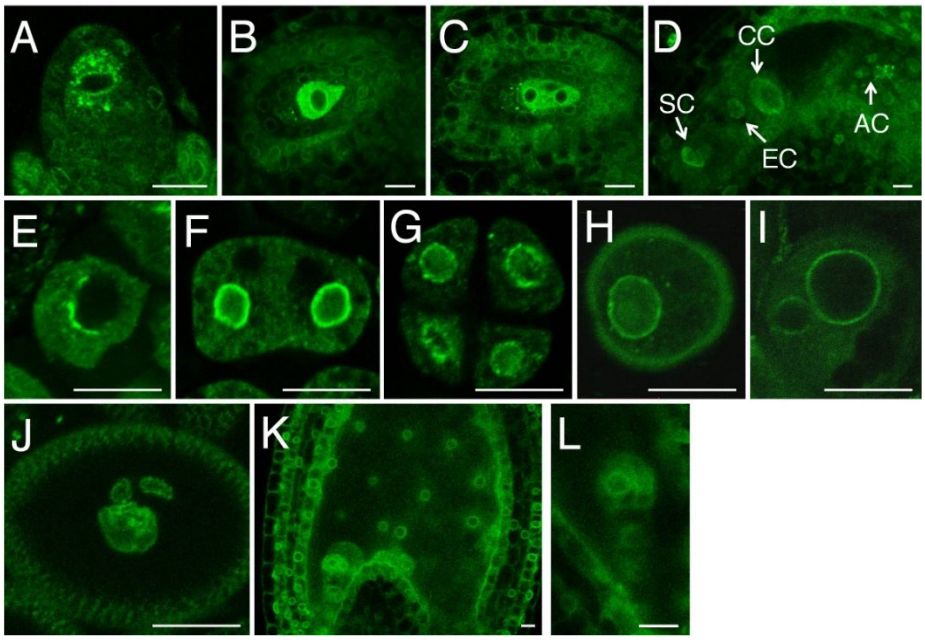

Figure 15. Representative images of the *Pro2.0kb:MOS7:GFP* expression during reproductive stages

A–D, Images of developing embryo sacs at MMC (A), FG1 stage (B), FG2 stage (C), and FG6 stage (D).

E–J, Images of developing pollen grains at PMC (E), dyad (F), tetrad (G), microspore (H), bicellular (I), and mature (tri-cellular, z-stack) pollen (J).

K, MOS7:GFP expression in seeds including embryo, endosperm and seed coat.

L, Close-up views of (K). Scale bars = 10 μm (A-L).

3.9 Dynein light chain and kinectin-related protein were identified as binding partners to MOS7 protein

Phenotypic analyses support the hypothesis that MOS7 is required in the reproductive stage of both female and male gamete formations. To clarify the function of MOS7 during reproductive stage in mitotic cells, I searched for MOS7-interacting proteins using Y2H assay. Fragmented N- and C-terminal domain of MOS7 protein were used for Y2H assay after screening, performed by Panbionet Corp. with *Arabidopsis* library (www.panbionet.com) (Figure 16A). The Y2H screen identified dynein light chain type 1 family protein and kinectin-related protein (Figure 16B). Dynein and kinesin are two well-known molecular motors, and kinectin serves as a receptor for kinesin (Vancoillie et al., 2000).

Using a mass spectrometry-based interactive proteomics with a Rae1-GFP tag, Tamura et al (2010) identified at least 30 *Arabidopsis* NUPs including MOS7. Thus, I checked MOS7 interaction with other NUPs, Rae1 and its binding partner Nup98a. I found that MOS7 interacts with Rae1 and Nup98a in yeast (Figure 16B).

Figure 16

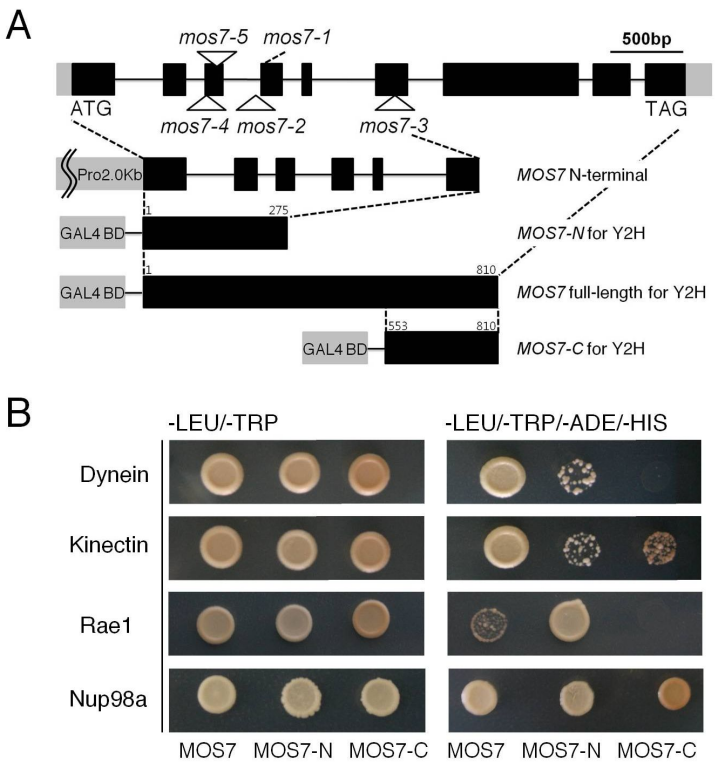

Figure 16. Dynein light chain and kinectin-related protein were identified as binding partners to MOS7 protein in Y2H assay

A, Three different *MOS7* cDNA fragments (Full-length *MOS7*, N-terminal *MOS7*, and C-terminal *MOS7*) were used as baits. Black box, translated exon; gray box, untranslated exon; line, intron.

B. MOS7 interaction with dynein light chain, kinectin-related protein, Rae1 and Nup98a was analyzed. All of the preys were used

with full-length cDNAs. -LEU/-TRP, complete medium minus leucine and tryptophan; -LEU/-TRP/-ADE/-HIS, complete medium minus leucine, tryptophan, adenine and histidine.

3.10 MOS7 binds to dynein light chain and kinectin-related protein *in vivo*

I investigated the *in vivo* interaction of full-length MOS7 with dynein light chain and kinectin-related protein in *Arabidopsis* protoplast using bimolecular fluorescence complementation (BiFC). I detected a strong reconstituted YFP signal in cytoplasmic region of the protoplast (Figure 17A).

Interestingly, I detected a strong reconstituted YFP fluorescence in the BiFC analysis between alpha tubulin and the two MOS7-interacting proteins found in Y2H screen, the dynein light chain and kinectin-related protein (Figure 17B). However, I was unable to detect a direct positive interaction between MOS7 and alpha tubulin (Figure 17C). Therefore, it is possible that MOS7 localizes at the mitotic microtubules via interaction with Rae1 and Nup98a or via interaction with dynein light chain and kinectin-related protein during cell division.

Figure 17.

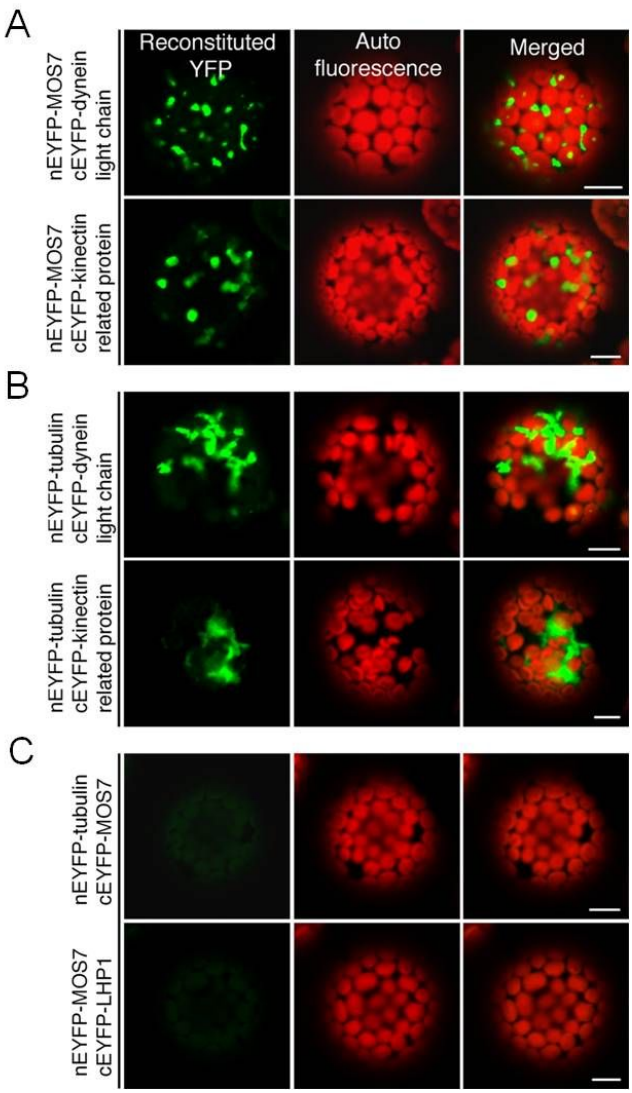

Figure 17. MOS7 binds to dynein light chain and kinectin-related protein *in vivo*

BiFC analysis for protein-protein interaction of MOS7 with dynein

light chain and kinectin-related protein (A), of dynein light chain and kinectin-related protein with tubulin (B), and of MOS7 with tubulin (C). Reconstituted YFP signal in the cytoplasmic region when two plasmids listed on the left were co-transfected in *Arabidopsis* cells.

C, Co-transfection of n*EYFP-MOS7* and *cEYFP-LHP1* was used as a negative control. Scale bars = 10 μm (A-C).

3.11 MOS7 localizes at the mitotic spindle structure during mitosis

Lee et al. (2009) reported that the Rae1 protein co-localizes with tubulin and binds directly to microtubules required for correct spindle assembly and chromosome segregation. Nup98 also interacts with microtubules and has a role in spindle assembly (Cross and Powers, 2011). Given that MOS7 interacts with Rae1 and Nup98a, it is possible that MOS7 might co-localize at the mitotic microtubules during cell divisions. The co-localization test of MOS7 protein and microtubule structures during mitosis are required to support my idea that MOS7 plays a critical role in regulation of microtubule dynamics via either its interaction with Rae1 and Nup98a or with dynein light chain and kinectin-related proteins. To address this hypothesis, I checked the localization of MOS7 and alpha tubulin using transgenic plants that express both GFP:TUA6 (green) and MOS7:RFP (red) proteins concurrently in dividing root tip cells. As the cells progressed into mitosis, I observed that MOS7 co-localized at the mitotic microtubule and the cell plate-forming zone until the end of cytokinesis (Figure 18, A, B, and C). After mitosis, MOS7 was found enriched at the newly

formed nuclear membrane (Figure 18D).

Figure 18.

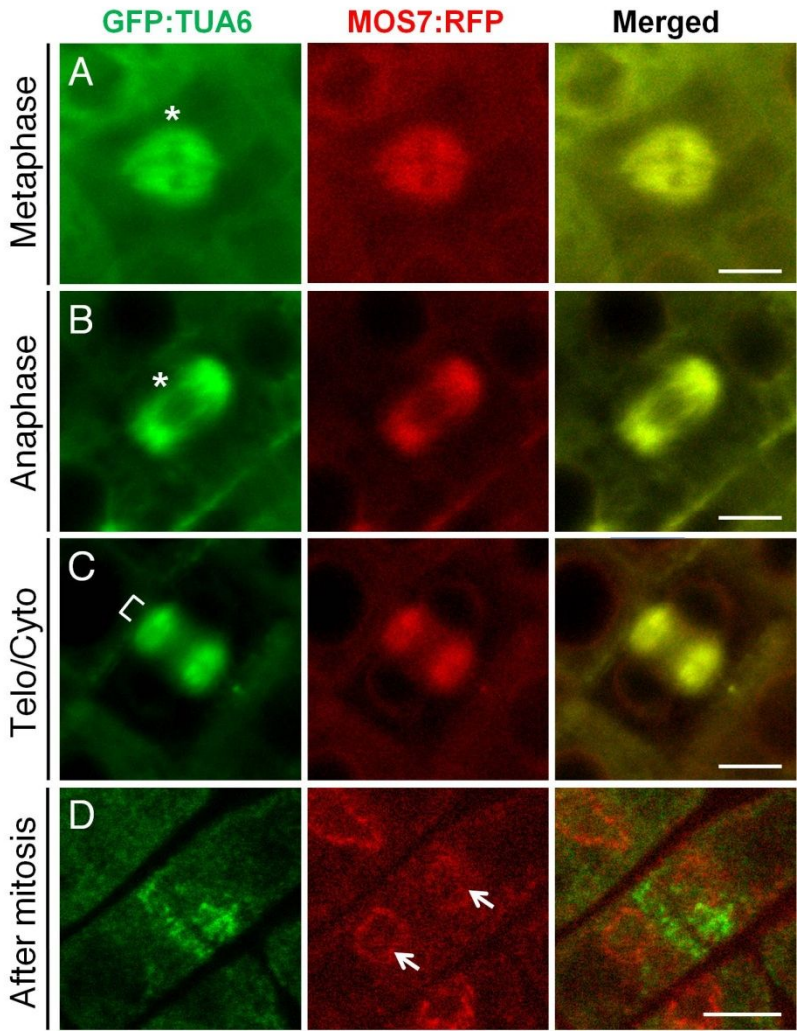

Figure 18. Association of MOS7 with microtubules during mitosis

All mitotic root cells are co-expressing GFP:TUA6 (left) and MOS7:RFP (middle) simultaneously at mitotic spindles and

phragmoplast structures. GFP:TUA6 indicates the different mitotic stages listed on the left. Scale bars = 5 μm.

A, Metaphase with spindle midzone (asterisk).

B, Anaphase with spindle midzone (asterisk).

C, Telophase with phragmoplast midline (bracket).

D, MOS7:RFP localization at newly formed nuclear membrane (arrows).

3.12 MOS7 modulates overall microtubule dynamics

Since MOS7 co-localized at the mitotic microtubule, this raises a possibility that a *mos7* mutant might show defects in microtubule dynamics due to dissociation or impaired binding to its interacting proteins. To determine this, I introduced the *ProUBQ14:GFP:TUA6* marker that expresses GFP-fused α-tubulin (Oh et al., 2010), and monitored microtubule dynamics at different developmental stages in male gametogenesis (Figure 19).

Prior to asymmetric division, the microspore nucleus migrates to the radial cell wall and is surrounded by a structured and directional array of cortical microtubules (Figure 19A). When the polarized microspore undergoes mitotic division, sister chromatids separate and are moved toward opposite poles by bipolar spindle microtubules (Figure 19B). Concurrently, interzonal microtubules rearrange into a bipolar phragmoplast array between the newly-forming two nuclei (Figure 19C). While phragmoplast microtubules gradually polymerize (Figure 19D) and encompass a small amount of cytoplasm containing the generative cell (Figure 19E), the cell plate forms at the midline of the phragmoplast (Figure 19M). Consequently, successful asymmetric division is determined by phragmoplast-mediated cell wall formation between a small lens-

shaped generative cell and a large vegetative cell (Figure 19M) (Lee et al., 2007).

In contrast, in half of the microspores from *mos7-5* heterozygous mutants, aberrant cortical microtubules were observed regardless of where the nucleus was positioned in the cytoplasm (Figure 19G). DAPI staining showed that the chromosomes were rather dispersed throughout the cytoplasm (Figure 19G) compared to those in wild-type (Figure 19A). Chromosomes were not segregated to the opposite poles (Figure 19, H, I, and J). Abnormal microtubule bundles were observed, and normal spindle assembly did not take place most of the time. The spindle assembly failed to attach to the sister chromatids correctly (Figure 19, H and I). Also, the phragmoplast did not form normally during the cell cycle progression (Figure 19J). Eventually, the microtubule bundles were lost or aberrantly localized in the cytoplasm (Figure 19K). Overall, MOS7 plays a pivotal role in microtubule dynamics including spindle assembly, spindle attachment to the kinetochore during karyokinesis and cell plate formation during cytokinesis.

Cell plate formation during PMI in *mos7-5* heterozygous plant was visualized using aniline blue staining, which detects callose in cell plates. While approximately half of the dividing microspores

showed normal callose deposition between the two newly-forming nuclei (Figure 19M), the other half displayed either branched or fragmented phragmoplasts. Therefore, the first mitotic division followed by cytokinesis and cell wall formation was perturbed (Figure 19N). The defects in microtubule dynamics and callose deposition that were observed in *mos7-5* mutants were more severe than those reported in γ-tubulin mutants (Zeng et al., 2009). Altogether, the data suggest that MOS7 plays a critical role in microtubule organization and dynamics during cell division.

Figure 19

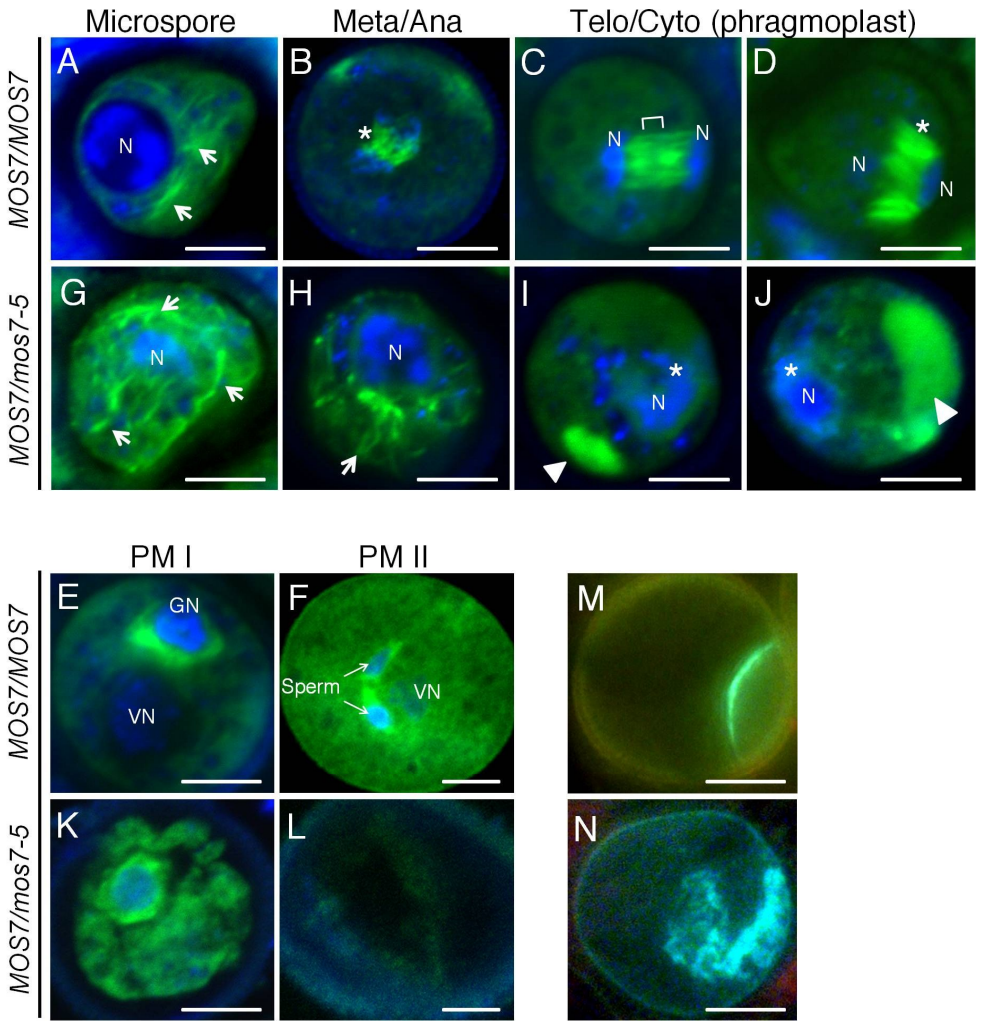

Figure 19. Defective microtubule dynamics during male gametogenesis in *MOS7/mos7-5* mutants

All images are composites of CLSM micrographs of *ProUBQ14:GFP:TUA6* expression merged with DAPI images (Green; GFP:TUA6, Blue; DAPI).

A–F, GFP:TUA6 expression in pollen grains from wild–type plants in different developmental stages.

A, Microspore with cortical microtubules (arrows).

B, Meta–Anaphase with spindle structure (asterisk).

C–D, Telophase with phragmoplast midline (bracket) and its polymerization (asterisk).

E, Bi–cellular stage.

F, Mature pollen grain.

G–L, GFP:TUA6 expression in pollen grains from *MOS7/mos7–5* mutants at the same growth period as that in wild–type A–F, respectively.

G, Microspore nucleus surrounded by cortical microtubules lacking orientation (arrows).

H, Defect in bi–polar microtubule configuration (arrow).

I–J, Failure of spindle assembly (arrowhead) and cytokinesis (asterisk).

K, Irregular microtubule accumulation in the cytoplasm.

L, Shrunken pollen grain.

M and N, Aniline blue–stained pollen grains at the bi–cellular stage.

M, Cell plate appearance in the middle of two cells after phragmoplast formation in wild–type.

N, Irregular and incomplete cell plate formation in the defective

pollen grains.

N, nucleus; GN, generative cell; VN, vegetative cell. Scale bars = 5 μm.

3.13 MOS7 also interacts with SAC pathway proteins in Yeast

As described previously, I searched for MOS7-interacting proteins using a Y2H library screening. The Y2H screen identified dynein light chain and kinectin-related protein, as well as Nup62, another nucleoporin protein (Figure 20A). During cell cycle progression, mitotic checkpoint complex (MCC) proteins localize to kinetochores and kinetochore microtubules, monitoring proper attachment of the bipolar spindle to the kinetochores of aligned sister chromatids (Musacchio and Salmon, 2007; Foley and Kapoor, 2013). Based on the observed *mos7-5* mutant phenotypes, it is possible that MOS7 might interact with MCC proteins. To check this possibility, I tested MOS7 interaction with three proteins that form a MCC: MAD2, BUB3 and BubR1. Among those, MOS7 bound to BubR1 in yeast (Figure 20B). Moreover, MOS7 also interacted with the *Arabidopsis* homologs of CDC20 (CDC20.1) and CCS52A1 (FZR2), the activating subunits of the anaphase promoting complex (APC) (Figure 19B). The cell cycle transition from metaphase to anaphase is induced by the APC, an E3 ubiquitin ligase that degrades cyclin B and securin (Pesin and Orr-Weaver, 2008). To prevent chromosome mis-segregation and aneuploidy, MCC

proteins and the Rae1-Nup98 complex sequester CDC20 and CCS52A1/FZR2 so that APC activity is inhibited until bi-orientation is achieved for all chromosomes (Jeganathan et al., 2005). Nup98 is also known as a Nup88-interacting protein in human (Griffis et al., 2003). So, I checked the binding of MOS7 to the Rae1 and Nup98 homologs of *Arabidopsis* and found positive interactions of MOS7 with both Rae1 and Nup98a (Figure 20B). In addition, I checked MOS7 binding to some APCs. The Y2H assay revealed that APC2, APC6, APC8 and APC10 were able to bind MOS7 in yeast (Figure 20C); Interestingly, mutations in those APCs resulted in a gametophytic lethality that can also be seen in the *mos7-5* mutant (Capron et al., 2003; Kwee and Sundaresan, 2003; Eloy et al., 2011; Zheng et al., 2011).

In this study, I expected that variation of the SAC signaling pathway could be possible by regulating APC/C activity through interaction with MCC proteins, Rae1 and Nup98 as well as APC/C family proteins. Failure in the SAC pathway often results in the early activation of APC and CyclinB degradation, causing unequal chromosome segregation and frequent aneuploidy (Gordon et al., 2012). However, the Cyclin B:GFP level was not likely altered and rare aneuploidy was observed in *MOS7/mos7-5* mutants (Figure 21, C and D), suggesting that APC activity was not changed. The

possible function of MOS7 binding to these proteins is discussed below.

Figure 20

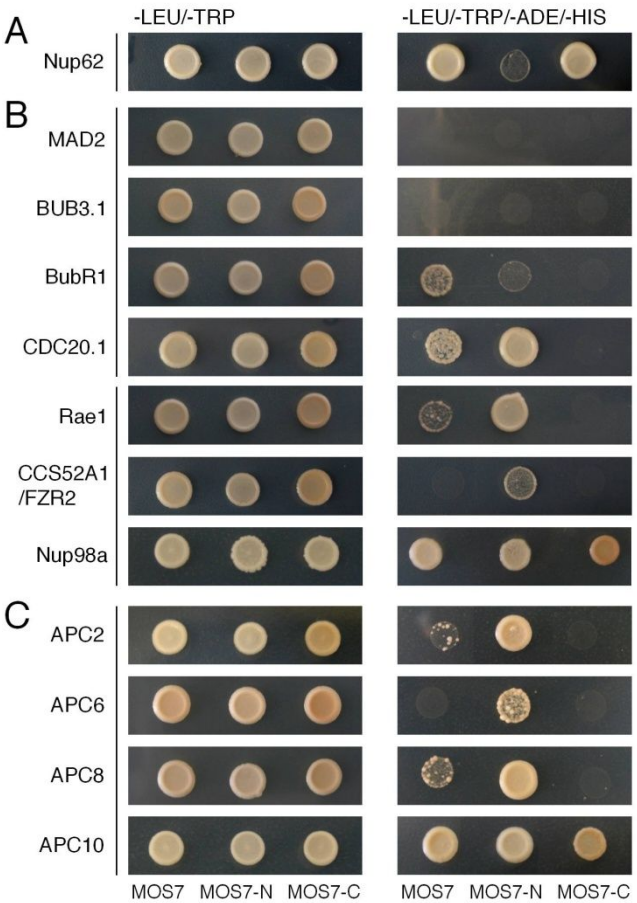

Figure 20. Interaction analysis of MOS7 protein in Y2H assay

A-C, Yeast two hybrid assay for interaction of MOS7.

Three different *MOS7* cDNA fragments as indicated in Figure 15A (Full-length MOS7, N-terminal MOS7, and C-terminal MOS7) were used as baits. MOS7 interaction to Nup62 nucleoporin (A), APC activity regulators including MCC (B)and four APCs (C) were

checked. Rae1 and Nup98 are also nucleoporins. All the preys were used with full-length cDNAs. -LEU/-TRP, complete medium minus leucine and tryptophan; -LEU/-TRP/-ADE/-HIS, complete medium minus leucine, tryptophan, adenine and histidine.

Figure 21

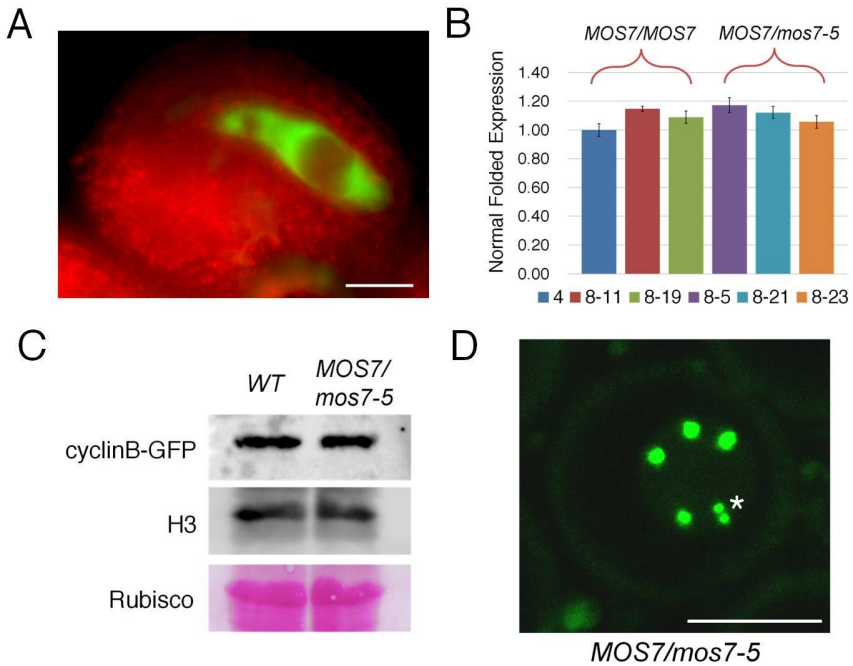

Figure 21. APC activity assay using *ProCYCB1;1:CYCB1;1:GFP* and *ProHTR12:HTR12:GFP* expression

A, Specific CYCB1;1:GFP protein expression was observed in the embryo sac (FG2 stage).

B, Expression level of *CYCB1;1:GFP* transgene using quantitative RT-PCR was checked and representative lines were selected for protein g blotting.

C, Protein gel blotting showing no difference of CYCB1;1:GFP protein level between wild-type and *MOS7/mos7-5*. H3 and

Ponceau S staining confirms equal loading.

D, A microspore with an extra chromosome (asterisk), a very rare aneuploidy in *MOS7/mos7-5* showing HTR12:GFP expression at 5+1 centromeres. *MOS7/MOS7* normal microspore is in Figure 3A. Scale bars = 25 μm (A), 10 μm in (D).

4. DISCUSSION

During interphase, NPCs are important multi-protein channels in the nuclear envelope (NE) responsible for macromolecular exchange between the nucleus and cytoplasm. However, in prophase, NPCs and NE disassemble during mitosis and the NUPs are distributed within the cytoplasm. Interestingly, active mitotic functions of NUPs have been assigned in a past few years in animals and vertebrates, with increased focus on the molecular mechanisms involved in the developmental process (Chatel and Fahrenkrog, 2011; Raices and D'Angelo, 2012).

The plant NPC contains at least 30 NUPs, some of which are homologous to NUPs in animals and yeast (Tamura et al., 2010). The individual functions of many of the plant NUPs are currently unknown. The purpose of this study was to explore the biological roles of the *Arabidopsis* nucleoporin MOS7, which is homologous to human Nup88, by examining the mutant phenotypes and protein interactions of MOS7.

The *mos7-1* mutant was first found from a suppressor screen of the *snc1* mutant. *snc1* mutant plants display both dwarf structure and constitutively-activated defense R protein (Cheng et al., 2009).

Although the *mos7-1* mutation rescued the defects caused by *snc1* mutation, *mos7-1* homozygous mutant showed no overt developmental phenotype. In this study, I used *mos7-2, mos7-3* and *mos7-4* alleles obtained from ABRC stock center, and I discovered a *mos7-5* allele by screening for seed set distortion. Through the study of these *mos7* mutants, I uncovered a role of MOS7 in mega- and microgametogenesis, and in embryogenesis.

4.1 Transmission of mutant *mos7-5* allele

In *MOS7/mos7-5* plants, many ovules and pollen grains were aborted before fertilization, and after fertilization, about 14% seeds were found aborted at the pre-globular stage. In a variety of ways, I confirmed that the aborted seeds were homozygous for the *mos7-5* allele: (1) No aborting seeds were produced when *mos7-5* or *mos7-3* heterozygous mutants were pollinated with wild-type pollen (Table 3). (2) Amplification of the T-DNA band was more than two-fold higher in aborting seeds than in heterozygous seedlings (Figure 9), and (3) 25% of the seeds were aborted in *mos7-3* heterozygous plants like recessive allele(Table 3). For gametogenesis, the data are more complex. 49% of the progeny showed ovule abortion (n=820) prior to fertilization when a *mos7-*

5 heterozygous plant was pollinated with wild-type pollen (Table 3). Considering that heterozygous females produce ovules in a ratio of 1 *MOS7* : 1 *mos7-5*, a likely hypothesis was that all of the aborted ovules were of the *mos7-5* genotype. And, I speculated that *mos7-5* allele could not be transmitted to the next generation because of co-segregation of *mos7-5* T-DNA with the abortion phenotype. However, when I genotyped the 244 progeny from the cross of a heterozygous *mos7-5* females with wild-type pollen, 110 plants were *mos7-5* heterozygous plants and 134 were wild-type plants. Transmission of the mutant *mos7-5* allele was not significantly different from that of the wild-type allele. The *mos7-5* allele is also clearly being transmitted through heterozygous males, although at a reduced rate from normal.

So, not all gamete cells carrying the wild-type allele survived. Likewise, not all gamete cells carrying the *mos7-5* mutant allele died (Figure 12). Inheriting the *mos7-5* mutant allele from the diploid MMC or PMC does not co-segregate with the abortion phenotype in the haploid cells. Instead, a haplo-insufficient scenario may explain the seeming contradiction of a high abortion rate along with a normal transmission rate. MOS7:GFP is clearly expressed in MMC and PMC (Figure 15, A and B). In a heterozygote, half of the normal amount of MOS7 might be produced

in MMC and PMC. As a result, half of the meiotic products (2 out of 4 cells) carrying over the MOS7 product would survive, whereas the other half of the meiotic products lacking the MOS7 product would die during the subsequent mitotic division, regardless of haploid genotype. Now, the pollen abortion phenotype appeared right after, but not during, microspore formation. This can be explained because nuclear division in meiosis I is not followed by cytokinesis (McCormick, 1993; Owen and Makaroff, 1995). Thus, functional, but haplo-insufficient, MOS7 proteins may contribute syncytial haploid cells that are alive during meiosis. Thereafter, only the haploid half that carries over the maternal MOS7 may survive. Considering that surviving meiotic products segregate independently after fertilization, I could expect 12.5% seed abortion because of zygotic lethality (Since the ratio of 4 (survived):4 (dead) was expected before fertilization, the ratio of 3(viable):1 (aborted) seeds could be expected after fertilization among four survived). Consistently, I observed the 3:1:4 segregation ratio of normal seeds, zygotic aborted seeds and gametophytic aborted ovules (Table 3). Perhaps, the level of maternally provided MOS7 decreases gradually and falls below the threshold right after meiosis or during subsequent mitotic divisions. This pattern is also seen in a cell-cycle dependent protein kinase, CDKA;1 protein, which is a

dosage-sensitive cell-cycle regulator carried over from maternal tissues (Liu et al., 2011; Zhao et al., 2012). If only half of the MOS7 protein is produced from MMC and PMC and if it localizes in the kinetochore or spindle pole, it would explain the abortion phenotype and the nearly-normal transmission of *mos7-5* mutant allele.

4.2 MOS7 functions during cell division through interaction with other proteins

NPCs typically form a distinct selective barrier between two compartments for nucleocytoplasmic transport in interphase cells. In addition, they are involved in dividing cells, as evidenced by mutations in some human and yeast NUPs causing mitotic defects, including incomplete cell division (Jeganathan et al., 2005; Zuccolo et al., 2007; Lussi et al., 2010; Mackay et al., 2010; Nakano et al., 2010; Chatel and Fahrenkrog, 2011). The observed defects are similar to those seen in *mos7-5* mutants. These findings indicate that some NUPs are functionally conserved in animal and plant cells during evolution.

The MOS7 Y2H screen and BiFC analysis identified two proteins that interact with MOS7, dynein light chain and kinectin-related protein. The *Arabidopsis* homologs of Rae1 and its interacting

partner Nup98 also bind to MOS7 in yeast, as well as BubR1, CDC20, CCS52A1/FZR2 and several APC proteins (APC2, APC6, APC8, APC10). All these proteins bind to the MOS7 N-terminus. Interestingly, full-length MOS7 failed to interact with prey constructs including APC2, APC6, APC8, Rae1, and CCS52A1, while N-terminal MOS7 domain is able to interact. Similar results have been reported previously, and it is a common problem with the Y2H assay that the conformation of an unpredictable full-length protein has a domain buried that then is not available to interact with other proteins (Deshaies, 1999; Chae et al., 2008; Bonetta, 2010). Thus, it is possible that an unoccupied C-terminal MOS7 in yeast may inhibit the N-terminal interaction with its partner or that the N-terminal MOS7 is accessible only when the C-terminal MOS7 interacts with other proteins. Nonetheless, the Rae1 interaction with MOS7 has already been detected successfully *in planta* (Tamura et al., 2010).

In human Nup88, the N-terminal domain is predicted to form a β-propeller structure that is important for nuclear protein complex assembly (Hashizume et al., 2010). Although homologous, the N-terminal two-thirds of the MOS7 protein showed no obvious structural motifs. Most of MOS7' s interactions with other proteins were through its N-terminal region (Figure 20), suggesting that the

N-terminus involvement in protein-protein interaction is conserved in animal and plant Nup88 homologs. The C-terminus of MOS7 is predicted to form a coiled-coil domain, related to the structural maintenance of chromosomes (SMC) family. I found that MOS7 can bind to Nup62 through C-terminal domain, and mutations in the MOS7 C-terminal region or *nup62* show similar defects in embryo formation (Figure 10).

Consistent with our Y2H result, immunoprecipitation and mass spectrometry have been used to show that MOS7 forms a Rae1 complex (Tamura et al., 2010). In this experiment, Nup98a was co-purified as a GFP-Rae1 binding protein. Blower et al. (2005) reported that the Rae1 protein localizes at the spindle aster and directly binds to microtubules required for spindle assembly organization. In plant cells, Rae1 co-localizes with tubulin and binds directly to microtubules *in vitro*, which is required for correct spindle assembly and chromosome segregation (Lee et al., 2009). Nup98 has a role in spindle assembly independent of Rae1. The binding of Nup98 to mitotic centromere-associated kinesin (MCAK), a microtubule-depolymerizing factor, is necessary for tubulin polymerization by inhibiting MCAK activity (Cross and Powers, 2011). These previous reports together with our MOS7-co-localization with tubulin data support the idea that that MOS7

protein might be involved in microtubule dynamics possibly through the interaction with Rae1 and Nup98a. Consistent with this, female gametophytic defects that are similar to the *mos7-5* mutant were also observed in *rae1* mutants (*Salk_030236*; Figure 22).

Consistent with our Y2H result, BiFC analysis showed that MOS7 can bind to the dynein light chain and the kinectin-related protein *in vivo* (Figure 17A). Surprisingly, no genes that encode homologs of the animal dynein heavy chain have been found in the *Arabidopsis* genome, and so the dynein light chain cannot assemble a conventional dynein motor (Wickstead and Gull, 2007). Also, the function of kinectin-related protein has not been characterized in *Arabidopsis*.

In HeLa cells, however, Rae1 binds to the nuclear mitotic apparatus (NuMA), which forms a complex with cytoplasmic dynein. Furthermore, interaction between Rae1 and NuMA coupled with dynein motor protein is critical for tethering microtubules at the spindle poles and is required for bipolar spindle formation (Merdes et al., 1996; Wong et al., 2006). It is tempting to speculate that the *Arabidopsis* dynein light chain interacts with unknown proteins to perform a function similar to that of the animal dynein. Consistent with this hypothesis, I found *in planta* interactions between tubulin and the dynein light chain or kinectin-related protein in the absence

of dynein heavy chain (Figure 17B). Future work will establish the functions of the dynein light chain and the kinectin-related protein found in our study during mitosis.

Since MOS7 can bind to Rae1, Nup98, and dynein, and since the balanced expression of *MOS7* is critical for seed viability, MOS7 might be involved in organizing overall spindle dynamics through N-terminal interaction with Rae1, Nup98 and dynein. In addition, MOS7 binds to MCC proteins, suggesting a role in the mitotic spindle checkpoint that is distinct from its role in interphase as a macromolecule channel such as a defense R protein (Cheng et al., 2009).

Rae1 and Nup98 have multiple, independent contributions in spindle assembly and in the SAC pathway by regulating APC/C activity. In the metaphase to anaphase transition, the ubiquitination of securin caused by the $APC^{CCS52A1/FZR2}$ regulator was inhibited by the Rae1 and Nup98 complex (Jeganathan et al., 2005). For anaphase onset, the extinction of SAC proteins occurred via dynein, which is implicated in the pole-ward transport of checkpoint proteins from kinetochores. The dynein located at the kinetochore is important in preventing aneuploidy and ensures faithful chromosome segregation (Foley and Kapoor, 2013).

In this study, I found that APC activity was not likely changed

(Figure 21). Alternatively, SAC extinction at the kinetochore proceeds through protein phosphatase 1 (PP1) targeting to kinetochore null protein 1 (KNL1), microtubule binding by KNL1, and dynein-dependent stripping of kinetochore proteins (Foley and Kapoor, 2013). The *mos7-5* mutant shows a distinct chromosome lagging phenotype. Perhaps *mos7-5* mutants cause defects in dynein-dependent stripping of kinetochore proteins, resulting in the chromosome lagging phenotype.

In addition, MOS7 can directly bind to APC and the APC-activating proteins. Interestingly, mutations in the MOS7-interacting APCs — *APC2, APC6, APC8* and *APC10* — showed a gametophytic lethality that can also be seen in the *mos7-5* mutant (Capron et al., 2003; Kwee and Sundaresan, 2003; Eloy et al., 2011; Zheng et al., 2011). Although there is no direct evidence yet, MOS7 might be directly involved in APC activity. Additional studies will provide further insights into the plant nucleoporin function during reproduction.

Figure 22

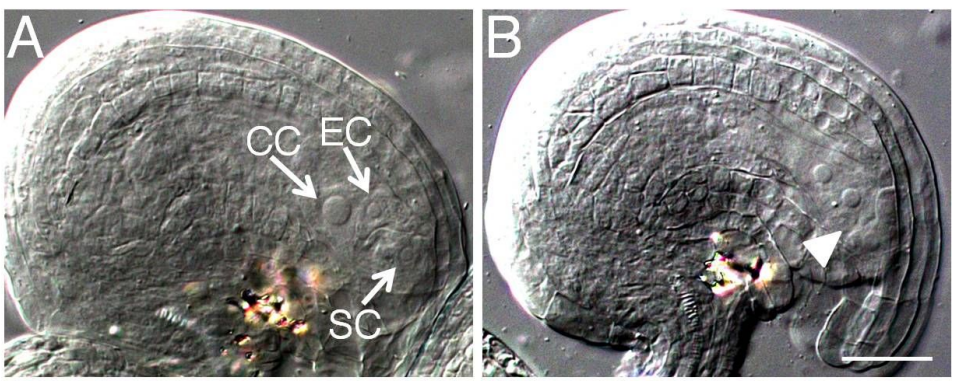

Figure 22. Defect in mitosis during female gametogenesis in *Rae1/rae1* mutant.

A and B, Mature ovules obtained from the same pistil of *Rae1/rae1* plant (*Salk_030236*).

A, Clearing of a normal ovule at the FG7 stage.

B, Developmental abnormality in *Rae1/rae1* ovule showing mitotic arrested embryo sac (arrowhead). Scale bar = 25 μm.

4.3 Dual functions of MOS7

4.3.1 MOS7 function in interphase

In snc1 (for suppressor of npr1-1, constitutive 1), a point mutation resulting in an E-to-K change in the linker region between the NB and LRR of an RPP4 homolog, renders this TIR-type R protein constitutively active without pathogen recognition (Zhang et al., 2003). As a consequence, snc1 mutant plants are dwarf, accumulate high levels of SA, and exhibit enhanced disease resistance against virulent pathogens (Li et al., 2001; Zhang et al., 2003). Cheng and colleagues note that autoimmunity of snc1 requires functional MOS7 since a partial loss of function mutation in *mos7-1* results in XPO1-mediated nuclear leakage of snc1 and suppression of all known snc1 auto-immune phenotypes (Cheng et al., 2009). MOS7 is required for appropriate nuclear accumulation of the auto-activated R protein snc1, as well as the downstream defense signaling components EDS1 and NPR1 (Figure 23A).

4.3.2 MOS7 function in mitosis

The past few years have unraveled that nucleoporins are also

important regulators of mitosis. Whilst for long time they were thought to remain latent in the mitotic cytoplasm, awaiting NPC reassembly, it is now accepted that nucleoporins are important for faithful cell division (Belgareh et al., 2001; Salina et al., 2003; Blower et al., 2005; Galy et al., 2006; Orjalo et al., 2006; Guttinger et al., 2009).

In this work, I also showed that *Arabidopsis* homolog of Nup88, MOS7, a nucleoporin and component of the NPC, has a critical function in mitotic division in reproductive stage including gametophytic and sporophytic development. Furthermore, MOS7 co-localizes at the microtubule structures during mitosis through interaction with several proteins described previously (Figure 23, B and C).

Localization of Rae1 reflects its association with mitotic MTs throughout mitosis (Lee et al., 2009). Histone H1 was shown to have microtubule-organizing activity in BY-2 cells and to promote microtubule nucleation through the formation of complexes with tubulin and the elongation of radial microtubules (Hotta et al., 2007; Nakayama et al., 2008). *Arabidopsis* TPX2 is actively exported in prophase from nucleus, enriched around the nuclear envelope, and then accumulates in the vicinity of the spindle (Vos et al., 2008). TPX2 also promotes spindle formation around chromosomes

through microtubule nucleation (Gruss and Vernos, 2004; Vos et al., 2008). Aurora kinases are associated with the outer nuclear membrane in prophase, and then gradually migrate to the spindle pole as mitosis progresses (Demidov et al., 2005). In metaphase, while Aurora associates with centromeric regions of chromosomes (Demidov et al., 2005), histone H1 re-localizes along the condensed chromosomes (Nakayama et al., 2008). γ-tubulin plays an essential role in microtubule nucleation, stabilization, and organization by binding to the minus end of microtubules(Job et al., 2003; Wiese and Zheng, 2006). *Arabidopsis* NEDD1 protein, which interacts with the γ-tubulin complex, decorates spindle microtubules and phragmoplast microtubules toward their minus ends (Zeng et al., 2009).

Figure 23

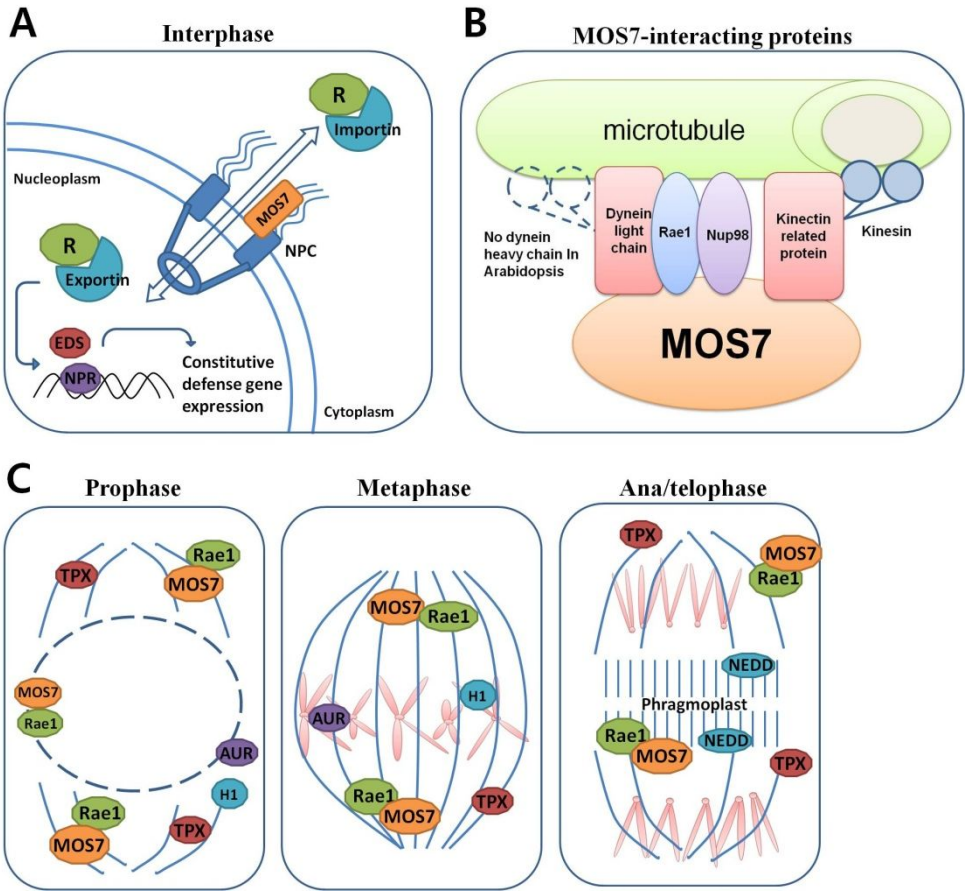

Figure 23. Dual functions of MOS7 during interphase and mitosis.

A, MOS7 localization on the cytoplasmic region of nuclear pore complex in interphase

B, MOS7 interacts with microtubules through making complex with dynein light chain, kinectin-related protein, Rae1 and Nup98.

C, Mitotic location of MOS7

4.4 MOS7 functions in somatic tissues

Because no homozygous *mos7* mutants could be acquired, the *MOS7* gene is most likely essential. Like *mos7* mutants, mutations in genes encoding proteins regulating microtubule organization often are homozygous lethal as reported (Park et al., 1998; Nakamura and Hashimoto, 2009). Fortunately, in *Arabidopsis*, meiotic cytokinesis takes place after karyokinesis processes are completed, so that haploid microspores carrying mutations in essential genes like *MOS7* are produced by heterozygous parents. Once the *mos7* microspores underwent cell division, the resulting gametophytic materials allowed me to analyze how mitosis might have been affected by the mutation.

In this work, functional study of MOS7 in somatic cell is almost impossible since no homozygous mutants were obtained in any of the mutant lines. Although, homozygous mutant of *mos7-1* allele, a partial MOS7-loss-of-function mutant (four amino acids in-frame deletion), were recovered by Cheng group, this mutant displays no developmental phenotypes since *mos7-1* allele still makes some functional MOS7 protein (Cheng et al., 2009).

Although sporophytic lethal mutation of *mos7* could not be brought to the homozygous status in somatic cells, I suspect that MOS7 have a critical function in somatic cell since microtubule-induced successful cell division is fundamental basis of growth in plant cell. Consistently, I detected MOS7-GUS/GFP signals in somatic cells including roots and leaves, as well as both gametophytes during reproductive development (Figure 14 and Figure 15).

I carried out q-PCR and established that the aborting seeds were homozygous for the *mos7-5* allele (Figure 9). Mutations in *MOS7* genes cause impaired mitotic divisions of seed, comprising diploid embryo and triploid endosperm. Considering the nearly-normal transmission of *mos7-5* mutant allele during gametogenesis, studies of mitosis and cytokinesis in *mos7* homozygous embryo/endosperm could be challenging cytological experiments in order to elucidate the function of MOS7 in somatic cells.

5. Conclusions

In this work, a genetic screen for seed-set distortion identified the *mos7-5* mutant. *MOS7* encodes an *Arabidopsis* Nup88 homolog,

a component of NPC. The results demonstrate that MOS7 is crucial for successful gametogenesis prior to fertilization and for embryogenesis after fertilization. MOS7 modulates overall microtubule dynamics including spindle assembly, spindle attachment to the kinetochore and phragmoplast formation during cell divisions, through protein–protein interaction with Rae1 and Nup98a and/or dynein light chain type 1 family protein and kinectin–related protein. Thus, this study provides insights into the plant NUPs' pivotal roles during mitosis in *Arabidopsis*.

6. Accession Numbers

Arabidopsis Genome Initiative numbers for the genes discussed in this study are as follows: *MOS7, At5g05680; MAD2, At3g25980; BUB3.1, At3g19590; BubR1, At2g33560; CCS52A1/FZR2, At4g22910; CDC20.1, At4g33270; APC2, At2g04460; APC6, AT1G78770; APC8, AT3G48150; ACP10, At2g18290; Kinectin–related protein, At2g17990; Dynein light chain type 1 family, At4g15930; Rae1, At1g80670; Nup98a, At1g10390; Nup62, At2g45000; CYCB1;1, At4g37490.*

REFERENCES

Allen JL, Douglas MG (1989) Organization of the nuclear pore complex in Saccharomyces cerevisiae. J Ultrastruct Mol Struct Res 102: 95-108

Belgareh N, Rabut G, Bai SW, van Overbeek M, Beaudouin J, Daigle N, Zatsepina OV, Pasteau F, Labas V, Fromont-Racine M, Ellenberg J, Doye V (2001) An evolutionarily conserved NPC subcomplex, which redistributes in part to kinetochores in mammalian cells. J Cell Biol 154: 1147-1160

Bernad R, Engelsma D, Sanderson H, Pickersgill H, Fornerod M (2006) Nup214-Nup88 nucleoporin subcomplex is required for CRM1-mediated 60 S preribosomal nuclear export. J Biol Chem 281: 19378-19386

Bernier G, Perilleux C (2005) A physiological overview of the genetics of flowering time control. Plant Biotechnol J 3: 3-16

Blower MD, Nachury M, Heald R, Weis K (2005) A Rae1-containing ribonucleoprotein complex is required for mitotic spindle assembly. Cell 121: 223-234

Bonetta L (2010) Protein-protein interactions: Interactome under

construction. Nature 468: 851-854

Braud C, Zheng W, Xiao W (2012) LONO1 encoding a nucleoporin is required for embryogenesis and seed viability in Arabidopsis. Plant Physiol 160: 823-836

Brohawn SG, Partridge JR, Whittle JR, Schwartz TU (2009) The nuclear pore complex has entered the atomic age. Structure 17: 1156-1168

Brohawn SG, Schwartz TU (2009) Molecular architecture of the Nup84-Nup145C-Sec13 edge element in the nuclear pore complex lattice. Nat Struct Mol Biol 16: 1173-1177

Brownell JE, Zhou J, Ranalli T, Kobayashi R, Edmondson DG, Roth SY, Allis CD (1996) Tetrahymena histone acetyltransferase A: a homolog to yeast Gcn5p linking histone acetylation to gene activation. Cell 84: 843-851

Brownfield L, Hafidh S, Durbarry A, Khatab H, Sidorova A, Doerner P, Twell D (2009) Arabidopsis DUO POLLEN3 is a key regulator of male germline development and embryogenesis. Plant Cell 21: 1940-1956

Canaday J, Stoppin-Mellet V, Mutterer J, Lambert AM, Schmit AC (2000) Higher plant cells: gamma-tubulin and microtubule nucleation in the absence of centrosomes. Microsc Res Tech 49: 487-495

Capron A, Serralbo O, Fulop K, Frugier F, Parmentier Y, Dong A, Lecureuil A, Guerche P, Kondorosi E, Scheres B, Genschik P (2003) The Arabidopsis anaphase-promoting complex or cyclosome: molecular and genetic characterization of the APC2 subunit. Plant Cell 15: 2370-2382

Cass DD, Peteya DJ, Robertson BL (1985) Megagametophyte development in *Hordeum vulgare*. 1. Early megagametogenesis and the nature of cell wall formation. Can. J. Bot. 63: 2164-2171

Chae E, Tan QK, Hill TA, Irish VF (2008) An Arabidopsis F-box protein acts as a transcriptional co-factor to regulate floral development. Development 135: 1235-1245

Chasan R, Walbot V (1993) Mechanisms of Plant Reproduction: Questions and Approaches. Plant Cell 5: 1139-1146

Chatel G, Fahrenkrog B (2011) Nucleoporins: leaving the nuclear pore complex for a successful mitosis. Cell Signal 23: 1555-1562

Cheng YT, Germain H, Wiermer M, Bi D, Xu F, Garcia AV, Wirthmueller L, Despres C, Parker JE, Zhang Y, Li X (2009) Nuclear pore complex component MOS7/Nup88 is required for innate immunity and nuclear accumulation of defense regulators in Arabidopsis. Plant Cell 21: 2503-2516

Christensen CA, Gorsich SW, Brown RH, Jones LG, Brown J, Shaw JM, Drews GN (2002) Mitochondrial GFA2 is required for synergid

cell death in Arabidopsis. Plant Cell **14:** 2215–2232

Christensen CA, King EJ, Jordan JR, Drews GN (1997) Megagametogenesis in *Arabidopsis* wild type and the Gf mutant. Sex. Plant Reprod. **10:** 49–64

Cross MK, Powers MA (2011) Nup98 regulates bipolar spindle assembly through association with microtubules and opposition of MCAK. Mol Biol Cell **22:** 661–672

Daigle N, Beaudouin J, Hartnell L, Imreh G, Hallberg E, Lippincott-Schwartz J, Ellenberg J (2001) Nuclear pore complexes form immobile networks and have a very low turnover in live mammalian cells. J Cell Biol **154:** 71–84

Demidov D, Van Damme D, Geelen D, Blattner FR, Houben A (2005) Identification and dynamics of two classes of aurora-like kinases in Arabidopsis and other plants. Plant Cell **17:** 836–848

Deshaies RJ (1999) SCF and Cullin/Ring H2-based ubiquitin ligases. Annu Rev Cell Dev Biol **15:** 435–467

Drews GN, Yadegari R (2002) Development and function of the Angiosperm female gametophyte. Annu. Rev. of Genetics **36:** 99–124

Dultz E, Zanin E, Wurzenberger C, Braun M, Rabut G, Sironi L, Ellenberg J (2008) Systematic kinetic analysis of mitotic dis- and reassembly of the nuclear pore in living cells. J Cell Biol **180:**

857-865

Elad N, Maimon T, Frenkiel-Krispin D, Lim RY, Medalia O (2009) Structural analysis of the nuclear pore complex by integrated approaches. Curr Opin Struct Biol 19: 226-232

Eloy NB, de Freitas Lima M, Van Damme D, Vanhaeren H, Gonzalez N, De Milde L, Hemerly AS, Beemster GT, Inze D, Ferreira PC (2011) The APC/C subunit 10 plays an essential role in cell proliferation during leaf development. Plant J 68: 351-363

Fang Y, Spector DL (2005) Centromere positioning and dynamics in living Arabidopsis plants. Mol Biol Cell 16: 5710-5718

Fiserova J, Kiseleva E, Goldberg MW (2009) Nuclear envelope and nuclear pore complex structure and organization in tobacco BY-2 cells. Plant J 59: 243-255

Foley EA, Kapoor TM (2013) Microtubule attachment and spindle assembly checkpoint signalling at the kinetochore. Nat Rev Mol Cell Biol 14: 25-37

Franz C, Walczak R, Yavuz S, Santarella R, Gentzel M, Askjaer P, Galy V, Hetzer M, Mattaj IW, Antonin W (2007) MEL-28/ELYS is required for the recruitment of nucleoporins to chromatin and postmitotic nuclear pore complex assembly. EMBO Rep 8: 165-172

Frosst P, Guan T, Subauste C, Hahn K, Gerace L (2002) Tpr is

localized within the nuclear basket of the pore complex and has a role in nuclear protein export. J Cell Biol **156:** 617–630

Galy V, Askjaer P, Franz C, Lopez-Iglesias C, Mattaj IW (2006) MEL-28, a novel nuclear-envelope and kinetochore protein essential for zygotic nuclear-envelope assembly in C. elegans. Curr Biol **16:** 1748–1756

Goldberg MW, Allen TD (1996) The nuclear pore complex and lamina: three-dimensional structures and interactions determined by field emission in-lens scanning electron microscopy. J Mol Biol **257:** 848–865

Gordon DJ, Resio B, Pellman D (2012) Causes and consequences of aneuploidy in cancer. Nat Rev Genet **13:** 189–203

Griffis ER, Xu S, Powers MA (2003) Nup98 localizes to both nuclear and cytoplasmic sides of the nuclear pore and binds to two distinct nucleoporin subcomplexes. Mol Biol Cell **14:** 600–610

Grini PE, Jurgens G, Hulskamp M (2002) Embryo and endosperm development is disrupted in the female gametophytic capulet mutants of Arabidopsis. Genetics **162:** 1911–1925

Gruss OJ, Vernos I (2004) The mechanism of spindle assembly: functions of Ran and its target TPX2. J Cell Biol **166:** 949–955

Guertin DA, Trautmann S, McCollum D (2002) Cytokinesis in eukaryotes. Microbiol Mol Biol Rev **66:** 155–178

Guttinger S, Laurell E, Kutay U (2009) Orchestrating nuclear envelope disassembly and reassembly during mitosis. Nat Rev Mol Cell Biol 10: 178-191

Hashizume C, Nakano H, Yoshida K, Wong RW (2010) Characterization of the role of the tumor marker Nup88 in mitosis. Mol Cancer 9: 119

Hotta T, Haraguchi T, Mizuno K (2007) A novel function of plant histone H1: microtubule nucleation and continuous plus end association. Cell Struct Funct 32: 79-87

Huang BQ, Sheridan WF (1994) Female Gametophyte Development in Maize: Microtubular Organization and Embryo Sac Polarity. Plant Cell 6: 845-861

Ingouff M, Hamamura Y, Gourgues M, Higashiyama T, Berger F (2007) Distinct dynamics of HISTONE3 variants between the two fertilization products in plants. Curr Biol 17: 1032-1037

Jeganathan KB, Malureanu L, van Deursen JM (2005) The Rae1-Nup98 complex prevents aneuploidy by inhibiting securin degradation. Nature 438: 1036-1039

Job D, Valiron O, Oakley B (2003) Microtubule nucleation. Curr Opin Cell Biol 15: 111-117

Johnston AJ, Matveeva E, Kirioukhova O, Grossniklaus U, Gruissem W (2008) A dynamic reciprocal RBR-PRC2 regulatory circuit

controls Arabidopsis gametophyte development. Curr Biol 18: 1680-1686

Johnston AJ, Meier P, Gheyselinck J, Wuest SE, Federer M, Schlagenhauf E, Becker JD, Grossniklaus U (2007) Genetic subtraction profiling identifies genes essential for Arabidopsis reproduction and reveals interaction between the female gametophyte and the maternal sporophyte. Genome Biol 8: R204

Joseph J, Liu ST, Jablonski SA, Yen TJ, Dasso M (2004) The RanGAP1-RanBP2 complex is essential for microtubule-kinetochore interactions in vivo. Curr Biol 14: 611-617

Kim HJ, Oh SA, Brownfield L, Hong SH, Ryu H, Hwang I, Twell D, Nam HG (2008) Control of plant germline proliferation by SCF(FBL17) degradation of cell cycle inhibitors. Nature 455: 1134-1137

Kwee HS, Sundaresan V (2003) The NOMEGA gene required for female gametophyte development encodes the putative APC6/CDC16 component of the Anaphase Promoting Complex in Arabidopsis. Plant J 36: 853-866

Lalanne E, Michaelidis C, Moore JM, Gagliano W, Johnson A, Patel R, Howden R, Vielle-Calzada JP, Grossniklaus U, Twell D (2004) Analysis of transposon insertion mutants highlights the diversity of mechanisms underlying male progamic development in Arabidopsis.

Genetics 167: 1975-1986

Lee JY, Lee HS, Wi SJ, Park KY, Schmit AC, Pai HS (2009) Dual functions of Nicotiana benthamiana Rae1 in interphase and mitosis. Plant J 59: 278-291

Lee YR, Li Y, Liu B (2007) Two Arabidopsis phragmoplast-associated kinesins play a critical role in cytokinesis during male gametogenesis. Plant Cell 19: 2595-2605

Li X, Clarke JD, Zhang Y, Dong X (2001) Activation of an EDS1-mediated R-gene pathway in the snc1 mutant leads to constitutive, NPR1-independent pathogen resistance. Mol Plant Microbe Interact 14: 1131-1139

Liu B, Ho CM, Lee YR (2011) Microtubule Reorganization during Mitosis and Cytokinesis: Lessons Learned from Developing Microgametophytes in Arabidopsis Thaliana. Front Plant Sci 2: 27

Loiodice I, Alves A, Rabut G, Van Overbeek M, Ellenberg J, Sibarita JB, Doye V (2004) The entire Nup107-160 complex, including three new members, is targeted as one entity to kinetochores in mitosis. Mol Biol Cell 15: 3333-3344

Lupu F, Alves A, Anderson K, Doye V, Lacy E (2008) Nuclear pore composition regulates neural stem/progenitor cell differentiation in the mouse embryo. Dev Cell 14: 831-842

Lussi YC, Shumaker DK, Shimi T, Fahrenkrog B (2010) The

nucleoporin Nup153 affects spindle checkpoint activity due to an association with Mad1. Nucleus 1: 71-84

Mackay DR, Makise M, Ullman KS (2010) Defects in nuclear pore assembly lead to activation of an Aurora B-mediated abscission checkpoint. J Cell Biol 191: 923-931

Matsuoka Y, Takagi M, Ban T, Miyazaki M, Yamamoto T, Kondo Y, Yoneda Y (1999) Identification and characterization of nuclear pore subcomplexes in mitotic extract of human somatic cells. Biochem Biophys Res Commun 254: 417-423

McCormick S (1993) Male Gametophyte Development. Plant Cell 5: 1265-1275

Meier I, Brkljacic J (2009) The nuclear pore and plant development. Curr Opin Plant Biol 12: 87-95

Meier I, Brkljacic J (2010) The Arabidopsis nuclear pore and nuclear envelope. Arabidopsis Book 8: e0139

Merdes A, Ramyar K, Vechio JD, Cleveland DW (1996) A complex of NuMA and cytoplasmic dynein is essential for mitotic spindle assembly. Cell 87: 447-458

Musacchio A, Salmon ED (2007) The spindle-assembly checkpoint in space and time. Nat Rev Mol Cell Biol 8: 379-393

Nakamura M, Hashimoto T (2009) A mutation in the Arabidopsis gamma-tubulin-containing complex causes helical growth and

abnormal microtubule branching. J Cell Sci **122:** 2208–2217

Nakano H, Funasaka T, Hashizume C, Wong RW (2010) Nucleoporin translocated promoter region (Tpr) associates with dynein complex, preventing chromosome lagging formation during mitosis. J Biol Chem **285:** 10841–10849

Nakano H, Wang W, Hashizume C, Funasaka T, Sato H, Wong RW (2011) Unexpected role of nucleoporins in coordination of cell cycle progression. Cell Cycle **10:** 425–433

Nakayama T, Ishii T, Hotta T, Mizuno K (2008) Radial microtubule organization by histone H1 on nuclei of cultured tobacco BY-2 cells. J Biol Chem **283:** 16632–16640

Oh SA, Allen T, Twell D (2010) A ticket for the live show: Microtubules in male gametophyte development. Plant Signal Behav **5**

Olmedo-Monfil V, Duran-Figueroa N, Arteaga-Vazquez M, Demesa-Arevalo E, Autran D, Grimanelli D, Slotkin RK, Martienssen RA, Vielle-Calzada JP (2010) Control of female gamete formation by a small RNA pathway in Arabidopsis. Nature **464:** 628–632

Onischenko E, Weis K (2011) Nuclear pore complex-a coat specifically tailored for the nuclear envelope. Curr Opin Cell Biol **23:** 293–301

Orjalo AV, Arnaoutov A, Shen Z, Boyarchuk Y, Zeitlin SG, Fontoura B, Briggs S, Dasso M, Forbes DJ (2006) The Nup107-160 nucleoporin complex is required for correct bipolar spindle assembly. Mol Biol Cell 17: 3806-3818

Owen HA, Makaroff CA (1995) Ultrastructure of microsporogenesis and microgametogenesis in Arabidopsis thaliana (L.) Heynh. ecotype Wassilewskija (Brassicaceae). Protoplasma 185: 7-21

Pagnussat GC, Yu HJ, Ngo QA, Rajani S, Mayalagu S, Johnson CS, Capron A, Xie LF, Ye D, Sundaresan V (2005) Genetic and molecular identification of genes required for female gametophyte development and function in Arabidopsis. Development 132: 603-614

Park SK, Howden R, Twell D (1998) The Arabidopsis thaliana gametophytic mutation gemini pollen1 disrupts microspore polarity, division asymmetry and pollen cell fate. Development 125: 3789-3799

Pastuglia M, Azimzadeh J, Goussot M, Camilleri C, Belcram K, Evrard JL, Schmit AC, Guerche P, Bouchez D (2006) Gamma-tubulin is essential for microtubule organization and development in Arabidopsis. Plant Cell 18: 1412-1425

Pesin JA, Orr-Weaver TL (2008) Regulation of APC/C Activators in Mitosis and Meiosis. Annu. Rev. Cell Dev. Biol. 24: 475-499

Pischke MS, Jones LG, Otsuga D, Fernandez DE, Drews GN, Sussman MR (2002) An Arabidopsis histidine kinase is essential for megagametogenesis. Proc Natl Acad Sci U S A 99: 15800-15805

Preuss D, Rhee SY, Davis RW (1994) Tetrad analysis possible in Arabidopsis with mutation of the QUARTET (QRT) genes. Science 264: 1458-1460

Raices M, D'Angelo MA (2012) Nuclear pore complex composition: a new regulator of tissue-specific and developmental functions. Nat Rev Mol Cell Biol 13: 687-699

Rasala BA, Orjalo AV, Shen Z, Briggs S, Forbes DJ (2006) ELYS is a dual nucleoporin/kinetochore protein required for nuclear pore assembly and proper cell division. Proc Natl Acad Sci U S A 103: 17801-17806

Roth P, Xylourgidis N, Sabri N, Uv A, Fornerod M, Samakovlis C (2003) The Drosophila nucleoporin DNup88 localizes DNup214 and CRM1 on the nuclear envelope and attenuates NES-mediated nuclear export. J Cell Biol 163: 701-706

Salina D, Enarson P, Rattner JB, Burke B (2003) Nup358 integrates nuclear envelope breakdown with kinetochore assembly. J Cell Biol 162: 991-1001

Schoft VK, Chumak N, Choi Y, Hannon M, Garcia-Aguilar M, Machlicova A, Slusarz L, Mosiolek M, Park JS, Park GT, Fischer RL,

Tamaru H (2011) Function of the DEMETER DNA glycosylase in the Arabidopsis thaliana male gametophyte. Proc Natl Acad Sci U S A 108: 8042-8047

Smith TF, Gaitatzes C, Saxena K, Neer EJ (1999) The WD repeat: a common architecture for diverse functions. Trends Biochem Sci 24: 181-185

Steffen JG, Kang IH, Macfarlane J, Drews GN (2007) Identification of genes expressed in the Arabidopsis female gametophyte. Plant J 51: 281-292

Strambio-De-Castillia C, Niepel M, Rout MP (2010) The nuclear pore complex: bridging nuclear transport and gene regulation. Nat Rev Mol Cell Biol 11: 490-501

Talbert PB, Masuelli R, Tyagi AP, Comai L, Henikoff S (2002) Centromeric localization and adaptive evolution of an Arabidopsis histone H3 variant. Plant Cell 14: 1053-1066

Tamura K, Fukao Y, Iwamoto M, Haraguchi T, Hara-Nishimura I (2010) Identification and characterization of nuclear pore complex components in Arabidopsis thaliana. Plant Cell 22: 4084-4097

Uv AE, Roth P, Xylourgidis N, Wickberg A, Cantera R, Samakovlis C (2000) members only encodes a Drosophila nucleoporin required for rel protein import and immune response activation. Genes Dev 14: 1945-1957

Vancoillie G, Lambert J, Mulder A, Koerten HK, Mommaas AM, Van Oostveldt P, Naeyaert JM (2000) Kinesin and kinectin can associate with the melanosomal surface and form a link with microtubules in normal human melanocytes. J Invest Dermatol 114: 421-429

Vos JW, Pieuchot L, Evrard JL, Janski N, Bergdoll M, de Ronde D, Perez LH, Sardon T, Vernos I, Schmit AC (2008) The plant TPX2 protein regulates prospindle assembly before nuclear envelope breakdown. Plant Cell 20: 2783-2797

Webb MC, Gunning BES (1994) Embryo Sac Development in Arabidopsis-Thaliana .2. The Cytoskeleton during Megagametogenesis. Sexual Plant Reproduction 7: 153-163

Weigel D, Ahn JH, Blazquez MA, Borevitz JO, Christensen SK, Fankhauser C, Ferrandiz C, Kardailsky I, Malancharuvil EJ, Neff MM, Nguyen JT, Sato S, Wang ZY, Xia Y, Dixon RA, Harrison MJ, Lamb CJ, Yanofsky MF, Chory J (2000) Activation tagging in Arabidopsis. Plant Physiol 122: 1003-1013

Wickstead B, Gull K (2007) Dyneins across eukaryotes: a comparative genomic analysis. Traffic 8: 1708-1721

Wiese C, Zheng Y (2006) Microtubule nucleation: gamma-tubulin and beyond. J Cell Sci 119: 4143-4153

Wong RW, Blobel G, Coutavas E (2006) Rae1 interaction with NuMA

is required for bipolar spindle formation. Proc Natl Acad Sci U S A **103:** 19783-19787

Xylourgidis N, Roth P, Sabri N, Tsarouhas V, Samakovlis C (2006) The nucleoporin Nup214 sequesters CRM1 at the nuclear rim and modulates NFkappaB activation in Drosophila. J Cell Sci **119:** 4409-4419

Yadegari R, Kinoshita T, Lotan O, Cohen G, Katz A, Choi Y, Nakashima K, Harada JJ, Goldberg RB, Fischer RL, Ohad N (2000) Mutations in the FIE and MEA genes that encode interacting polycomb proteins cause parent-of-origin effects on seed development by distinct mechanisms. Plant Cell **12:** 2367-2381

Yang CY, Spielman M, Coles JP, Li Y, Ghelani S, Bourdon V, Brown RC, Lemmon BE, Scott RJ, Dickinson HG (2003) TETRASPORE encodes a kinesin required for male meiotic cytokinesis in Arabidopsis. Plant J **34:** 229-240

Zeng CJ, Lee YR, Liu B (2009) The WD40 repeat protein NEDD1 functions in microtubule organization during cell division in Arabidopsis thaliana. Plant Cell **21:** 1129-1140

Zeng CJT, Lee Y-RJ, Liu B (2009) The WD40 Repeat Protein NEDD1 Functions in Microtubule Organization during Cell Division in Arabidopsis thaliana. Plant Cell **21:** 1129 1140

Zhang Y, Goritschnig S, Dong X, Li X (2003) A gain-of-function

mutation in a plant disease resistance gene leads to constitutive activation of downstream signal transduction pathways in suppressor of npr1-1, constitutive 1. Plant Cell 15: 2636-2646

Zhao X, Harashima H, Dissmeyer N, Pusch S, Weimer AK, Bramsiepe J, Bouyer D, Rademacher S, Nowack MK, Novak B, Sprunck S, Schnittger A (2012) A general G1/S-phase cell-cycle control module in the flowering plant Arabidopsis thaliana. PLoS Genet 8: e1002847

Zheng B, Chen X, McCormick S (2011) The anaphase-promoting complex is a dual integrator that regulates both MicroRNA-mediated transcriptional regulation of cyclin B1 and degradation of Cyclin B1 during Arabidopsis male gametophyte development. Plant Cell 23: 1033-1046

Zuccolo M, Alves A, Galy V, Bolhy S, Formstecher E, Racine V, Sibarita JB, Fukagawa T, Shiekhattar R, Yen T, Doye V (2007) The human Nup107-160 nuclear pore subcomplex contributes to proper kinetochore functions. EMBO J 26: 1853-1864

ABSTRACT IN KOREAN

애기장대와 같은 고등한 식물에서는 유전정보의 차별화된 발현이 식물의 생활사에 필수적이다. 동물과는 다르게 식물은 포자체(sporophyte)와 배우체(gametophyte)의 세대교번이 일어난다. 십수 년 이상 배우자(gamete), 배아(embryo), 배젖(endosperm)의 발달단계를 포함하는 생식과정(reproductive stage)에서 발현하는 유전자들이 수많이 밝혀져 왔다. 하지만, 이러한 관련 유전자들이 생식과정에서 어떻게 상호작용 하는지에 관한 연구는 현재까지 매우 제한적이다. 따라서 본 학위논문은 모델식물 애기장대를 이용하여 배우자와 종자 발달단계의 분자적 상호작용과 조절기작을 이해하는데 초점을 두었다.

이번 연구에서는 배우자와 종자형성과정에서 유산되는 표현형을 보이는 *mos7-5* 돌연변이체를 획득하게 되었다. *MOS7(Modifier Of Snc1,7)*은 인간의 핵공단백질88(Nucleoporin88)과 유사성이 높은 애기장대의 핵공단백질을 암호화 한다. *mos7-5* 돌연변이는 열성(recessive)의 기능결손(loss-of-function) 돌연변이이고 동형접합체(homozygote)의 생성이 불가능하기 때문에 이형접합체(heterozygote)로 세대유지가 가능하다. *mos7-5* 이형접합돌연변이체는 자성배우자형성(megagametogenesis)과정에서 유사분열(mitosis)의 결함으로 인해 FG2 단계이상 진행하지 못하고 약

48%의 배낭(embryo sac)의 발달에 문제가 생긴다. 비슷하게 웅성배우자형성(microgametogenesis) 과정에서도 유사분열에 결함이 생긴다. 또한 반가불충분성(haplo-insufficient)의 특성이 있으나 감수분열(meiosis)시에는 표현형이 나타나지 않고 유사분열을 하는 시기에 표현형이 나타나게 된다. 수정 이후에는 약 14%의 종자 유산이 확인되는데 PCR을 통해 유산된 종자들이 *mos7-5*의 동형접합체임을 확인하였다. 효모단백질잡종선별법(Yeast two hybrid screening)을 통해 dynein light chain type 1 family와 kinectin-related 단백질과의 결합을 확인하였고 이분자형광상보성 (BiFC)실험으로 식물세포 내 결합을 한번 더 검증할 수 있었다. 게다가 미세소관 역학의 조절에 기능을 하는 것으로 알려진 핵막단백질 Rae1, Nup98과의 결합도 효모단백질잡종선별법으로 확인하였다. 형광 (fluorescence)과 공초점현미경 (confocal microscope)을 이용한 분석에서 세포의 유사분열시기에는 MOS7 단백질이 방추사(spindle) 구조물에 위치하는 것을 확인할 수 있었고, 미세소관 추적 및 분석을 통해 배우자형성(gametogenesis)과정 동안 *mos7-5* 돌연변이체에서는 전체적인 미세소관의 역학, 특히 방추사의 조립(assembly)과 방추사의 동원체(kinetochore) 부착, 격막형성체(phragmoplast)의 형성 등에 결함이 생기는 것을 알 수 있었다. 이러한 결과들로 미루어 볼 때 MOS7은 세포분열시 Rae1, Nup98, dynein light chain, kinectin-related 단백질과의 결합 및 상호작용을 통해 미세소관 역학을 조절하는 것으로 추측된다. 또한 미세소관의 역동성 조절은 식물의 발달과정

전반에 걸쳐 필수적인 요소이고 MOS7이 광범위한 조직, 세포유형에서 발현된다는 것으로 미루어 볼 때, MOS7의 기능이 배우자 형성과정뿐 아니라 체세포(somatic cell)에서 작동함을 유추할 수 있다. 본 연구는 애기장대의 MOS7이 세포분열에 있어서 필수적인 역할을 한다는 것을 뒷받침 한다.

주요어: 배우자형성과정, 핵공복합체, 핵막단백질, 미세소관 역학, 유사분열

학번: 2007-20345